

NASA CR-112032

# ELECTRONICALLY TUNED OPTICAL FILTERS

BY

JOSEPH A. CASTELLANO, EDWARD F. PASIERB, CHAN S. OH,  
AND MICHAEL T. McCaffrey

CASE FILE  
COPY

JANUARY 1972

PREPARED UNDER CONTRACT NO. NAS 1-10490

RCA LABORATORIES  
PRINCETON, NEW JERSEY 08540

LANGLEY RESEARCH CENTER  
NATIONAL AERONAUTICS AND SPACE ADMINISTRATION  
HAMPTON, VIRGINIA 23365



# **ELECTRONICALLY TUNED OPTICAL FILTERS**

BY

JOSEPH A. CASTELLANO, EDWARD F. PASIERB, CHAN S. OH,  
AND MICHAEL T. McCaffrey

**JANUARY 1972**

PREPARED UNDER CONTRACT NO. NAS 1-10490

RCA LABORATORIES  
PRINCETON, NEW JERSEY 08540

LANGLEY RESEARCH CENTER  
NATIONAL AERONAUTICS AND SPACE ADMINISTRATION  
HAMPTON, VIRGINIA 23365



## TABLE OF CONTENTS

Section	Page
I. INTRODUCTION .....	2
A. Background .....	2
B. Discussion .....	2
II. ELECTRONIC COLOR SWITCHING .....	3
A. Materials .....	3
1. Nematic Hosts .....	3
2. Pleochroic Dyes .....	4
B. Electro-Optic Behavior .....	5
1. Spectral Response .....	5
2. Material and Device Properties .....	9
3. Response Time Characteristics .....	9
4. Life Tests .....	10
III. FIELD-INDUCED PHASE CHANGES .....	10
A. Materials .....	10
B. Electro-Optic Behavior .....	16
1. Field Dependence .....	17
2. Light-Scattering Characteristics .....	19
3. Response Time Characteristics .....	25
4. Device Thickness .....	31
5. Temperature Effects .....	31
6. Device Evaluation .....	31
IV. STATE-OF-THE-ART DEVICES .....	32
A. Electronically Controlled Color Filter .....	32
B. Simulated Aircraft Engine-Monitoring System .....	38
REFERENCES .....	42
NEW TECHNOLOGY APPENDIX .....	43



## LIST OF ILLUSTRATIONS

Figure	Page
1. Optical absorption spectrum of yellow dye in PEBAB-RT .....	6
2. Optical absorption spectrum of mixture of indophenol blue and PNAZA in PEBAB-RT .....	7
3. Optical absorption spectrum of magenta dye in PEBAB-RT .....	8
4. Phase transition plot of series: $C_2H_5CH(CH_3)(CH_2)_nOC_6H_4CHNC_6H_4CN...$ .....	14
5. Phase diagram of binary mixture of CH-1 in PEBAB-RT .....	15
6. Relative brightness vs. voltage for four different mixtures .....	18
7. Experimental arrangement for measuring light scattering of liquid crystal cells .....	19
8. Scattering intensity vs. detector angle .....	21
9. Angular dependence of contrast ratio as a function of incidence angle, (40% CH-1 mixture) .....	22
10. Angular dependence of contrast ratio as a function of incidence angle, (60% CH-1 mixture) .....	23
11. Contrast improvement using crossed polarizers. 40% CH-1, ½ mil cell, detector angle = 0° .....	24
12. Response time (dc) as observed with crossed polarizers .....	26
13. Response time (dc) as observed with crossed polarizers .....	27
14. AC response time as observed with crossed polarizers .....	28
15. Two-step electro-optic relaxation characteristic .....	29
16. Relaxation time as observed with crossed polarizers, ½ mil cells, incidence angle = 0°, detector angle = 0° .....	30
17. Top and edge view of two stacked color cells .....	34
18. Color pattern of electronically activated two-layer polychromic filter .....	35
19. Two-layer electronically controlled color filter .....	36



## LIST OF ILLUSTRATIONS (Continued)

Figure	Page
20. Schematic diagram of polychromic filter .....	36
21. Relative radiant output energy and luminosity curves vs. wavelength .....	37
22. Top view of bar-graph display .....	39
23. Cross-sectional view of segmented column .....	39
24. Electrical addressing scheme for 3-column bar-graph.....	41



## ELECTRONICALLY TUNED OPTICAL FILTERS

By Joseph A. Castellano, Edward F. Pasierb, Chan S. Oh  
and Michael T. McCaffrey

### SUMMARY

Research on electro-optic effects based on guest-host interactions in liquid crystals is described. The development of a three-color, subtractive display based on electronic color switching materials was attempted. Several prototype three-layer stacked arrays were fabricated and tested during the current reporting period. Primary effort was concentrated on compromising some of the more serious problems encountered and described in our previous technical reports (Ref. 1, 2). Unfortunately, the problems of magenta dye stability, color uniformity and parallax could not be satisfactorily overcome. As a result a two-layer polychromic filter was constructed. This device consisted of two separate color cells containing pleochroic dye molecules that transmit either cyan or yellow. In combination, four different colors are produced by electronic control of the individual cells.

The synthesis of new nonsteroidal, cholesteric liquid crystals was accomplished during the report period. One compound from this series exhibited a cholesteric range from 48 to 66°C. This compound in a mixture with room-temperature nematic materials exhibited field-induced phase changes at much lower voltages than previously observed for steroidal type compounds. One formulation had a cholesteric range of 0° to 75°C and exhibited helical unwinding from the opaque cholesteric state to the clear nematic state in 100 msec at 30 V. Relaxation of the molecules to the original opaque state was a complex two-step process, which required 150 msec.

Efforts to apply these field-induced phase change effects to practical display devices resulted in the construction of a simulated aircraft engine-monitoring indicator. This bar-graph display has a total of 36 elements in three bars. As each succeeding element in any one bar is activated, the material becomes clear and the engine operating parameter appears.



## I. INTRODUCTION

### A. Background

This report is a detailed account of our efforts to develop a three-layer, polychromic filter that can be tuned electronically. The operation of the filter is based on the cooperative alignment of pleochroic dye molecules by nematic liquid crystals activated by electric fields. This orientational effect produces changes in the optical density of the material and thus changes in the color of light transmitted through the medium. Hence, this effect has been termed "electronic color switching."

During the first two years of our contract with NASA (Refs. 1,2), we developed nematic materials and pleochroic dyes which permitted operation of a variety of electronically tuned filters over a broad temperature range. Research conducted during the past year (January 1, 1971 to December 31, 1971) was largely devoted to the development of a subtractive, three-layer cell structure which permits electronic tuning over a broad spectral range.

In addition to the work on electronic color switching this report describes our efforts to develop improved materials and devices which employ field-induced changes of a cholesteric to a nematic liquid crystal. The process occurs as a result of a breakdown of the helical structure characteristic of the cholesteric state, i.e., a finite pitch system transformed into a system of infinite pitch. When the field is removed the system reverts back to its helical structure. Thus, the material changes from an opaque or light-scattering state (cholesteric) to a clear state (homeotropic nematic) by application of an externally applied electric field.

The materials which we prepared for the field-induced phase change studies were nonsteroidal cholesteric compounds. Because of their lower viscosity characteristics in comparison with those of the steroidal esters, these compounds required lower voltage and operated at higher speeds than the previously reported materials.

This research was conducted in the Communications Research Laboratory, K. H. Powers, Director, with J. A. Castellano as Project Scientist and D. A. Ross as Project Supervisor. E. F. Pasierb, C. S. Oh, and M. T. McCaffrey also contributed to the effort during the report period.

### B. Discussion

The effect of electric fields on various mixtures of pleochroic dyes and nematic host compounds has been extensively studied under NASA contract (Refs. 1,2). This research

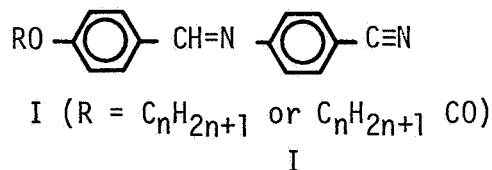
led to the development of nematic host materials with broad operating temperature ranges. In addition, we prepared a series of dye-liquid crystal systems which gave a wide variety of color changes upon application of electric fields. A considerable effort was also expended in the design and development of a three-color stacked array which would ultimately control the color of light throughout the visible portion of the spectrum. In Section II of this report we will describe our efforts to fabricate a working model of this display device.

Section III of this report concerns itself with research directed toward developing new materials for field-induced phase change studies. Previous studies involved the use of steroidal cholesteric compounds which operated at rather high voltages (Ref. 3). The use of nonsteroidal cholesteric materials was also reported (Ref. 4), but high operating voltages and temperatures were required to observe the effect. Our work under this contract has been largely devoted to the preparation of nonsteroidal cholesteric compounds which operate at low voltages and over a broad temperature range.

## II. ELECTRONIC COLOR SWITCHING

### A. Materials

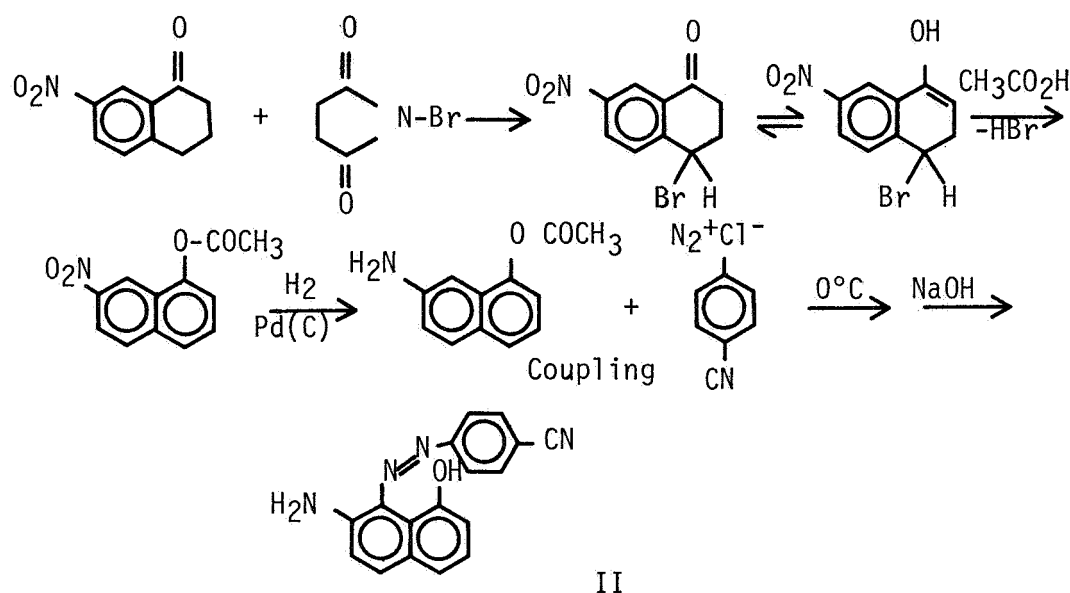
1. Nematic Hosts — An extensive investigation of structure-property relationships was previously carried out (Refs. 1,2) and resulted in the development of a stable nematic mixture with a broad operating temperature range (Ref. 1). The mixture, referred to as PEBAB-RT, consists of compounds with the general structure I. The cyano group ( $C \equiv N$ ) in the terminal position of the molecules produces a strong dipole moment along the



molecular axis. This property enables the molecules to orient with their long axes in the direction of externally applied electric fields and thus to produce cooperative alignment of dissolved pleochroic dye molecules. Since no new work was done on the synthesis of host materials, PEBAB-RT was used as the nematic host in all of our electro-optic studies.



2. Pleochroic Dyes — During the past year an extensive effort was made to prepare modest quantities of a stable, magenta dye which had pleochroic properties. One such compound is the azo dye with structure II which was prepared by the following series of reactions:



Initial attempts at synthesis of II resulted in a product with a melting point which was considerably lower than the reported value (Ref. 5) and which did not exhibit the desired pleochroic properties. Thin layer chromatography of the purified products after each step showed that the synthesis was progressing as planned up to the coupling reaction with p-cyanophenyldiazonium chloride. Initially, the coupling was carried out in a buffered solution at pH 4-5 according to the original preparation (Ref. 5). However, the majority of the diazonium salts used by Ross and Reissner bore electron donating substituents, and this buffered solution prevented acid-catalyzed decomposition as well as giving the maximum coupling rate. Although these authors state that the procedure may also be used with salts bearing electron-withdrawing groups our attempts at obtaining the desired product in a purified state were unsuccessful.

It was therefore decided to perform the coupling at a pH of 1-2. This resulted in the formation of the desired compound in a pure state. However, the material was not stable for extended periods, and after about four weeks changes in its absorption spectrum were noted. Air oxidation of the compound through the free amine function is probably responsible for the formation of colored decomposition products. Future work on this series of dyes should involve the use of various substituents on the amino group to block this oxidation.

## B. Electro-Optic Behavior

1. Spectral Response — Since the observed color qualities of the pleochroic dye molecules are due to optical absorption characteristics, maximum efficiency for an all-color optical filter can best be accomplished using transmitted light through guest-host materials which exhibit the primary subtractive colors: cyan, magenta, and yellow. The range of colors which can be produced by these three dyes is quite large and makes possible the modern processes of color photography and printing which depend on the subtractive principle. In all such processes, the real function of the subtractive primaries is to control the red, green, and blue light to which the three visual receptor systems are sensitive. Thus, cyan, which subtracts red light from white light, is used in various proportions to control the amount of red light reaching the eye. Similarly, magenta and yellow are used to control green and blue light, respectively.

Earlier experimental studies have been directed toward the preparation and development of room-temperature liquid crystalline compounds and selected pleochroic dyes exhibiting the color characteristics of the subtractive primary colors yellow and cyan (Refs. 1,2). Figures 1 and 2 show the optical absorption characteristics of two cells containing the selected dye materials dissolved in PEBAB-RT nematic material. The darkened area in each figure illustrates the absorption characteristics of the Kodak Wratten filter corresponding to the desired primary color. Ideally, the absorption spectrum of the electro-optic cell and the comparative Kodak filter should be closely matched for maximum color range and selectivity. The ability of each individual color cell to be electronically switched to a colorless state determines the brightness and color saturation capabilities of the composite unit.

The successful synthesis of a pleochroic magenta dye (Structure II) compatible with our PEBAB-RT nematic host material allowed tests to be made to determine the effects of dye concentration and cell thickness on optical absorption characteristics. Optimum color contrast of a 0.5-mil-thick parallel plate cell occurred at  $\sim 1.0\%$  concentration of the magenta dye. Figure 3 shows that the absorption spectrum of such a cell in a room-temperature nematic host approximates that of Kodak Wratten filter #32 (magenta). Greater concentrations reduced the color contrast ratio while lesser amounts did not allow complete saturation of the color characteristics.

This particular attribute of color saturation is essential if a variable color filter is to be produced. Insufficient color contrast available from the magenta cell is one of the principal reasons a tri-color stacked array using materials that transmit the true primary subtractive colors could not be successfully fabricated.



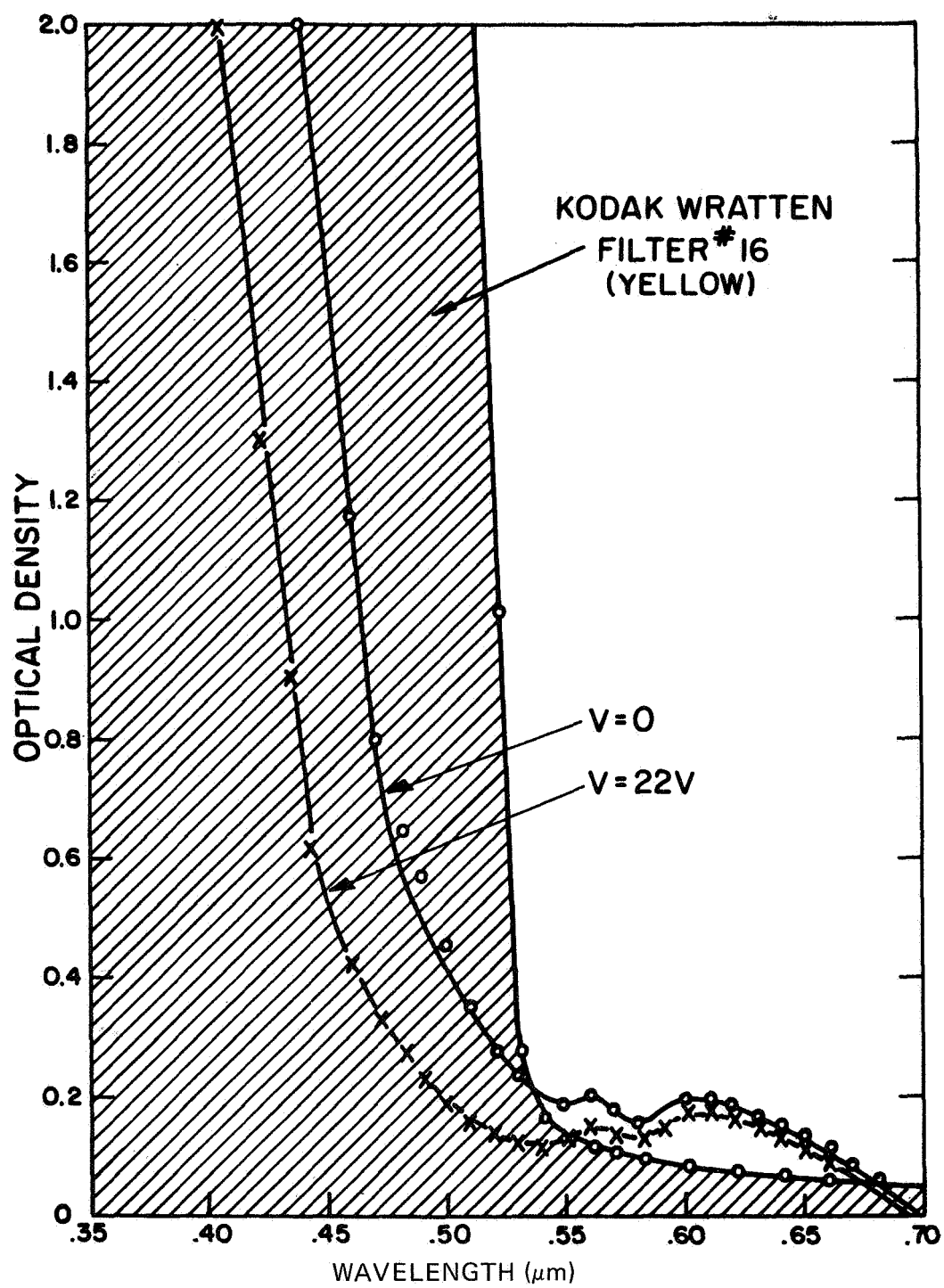


Figure 1. Optical absorption spectrum of yellow dye in PEBAB-RT.

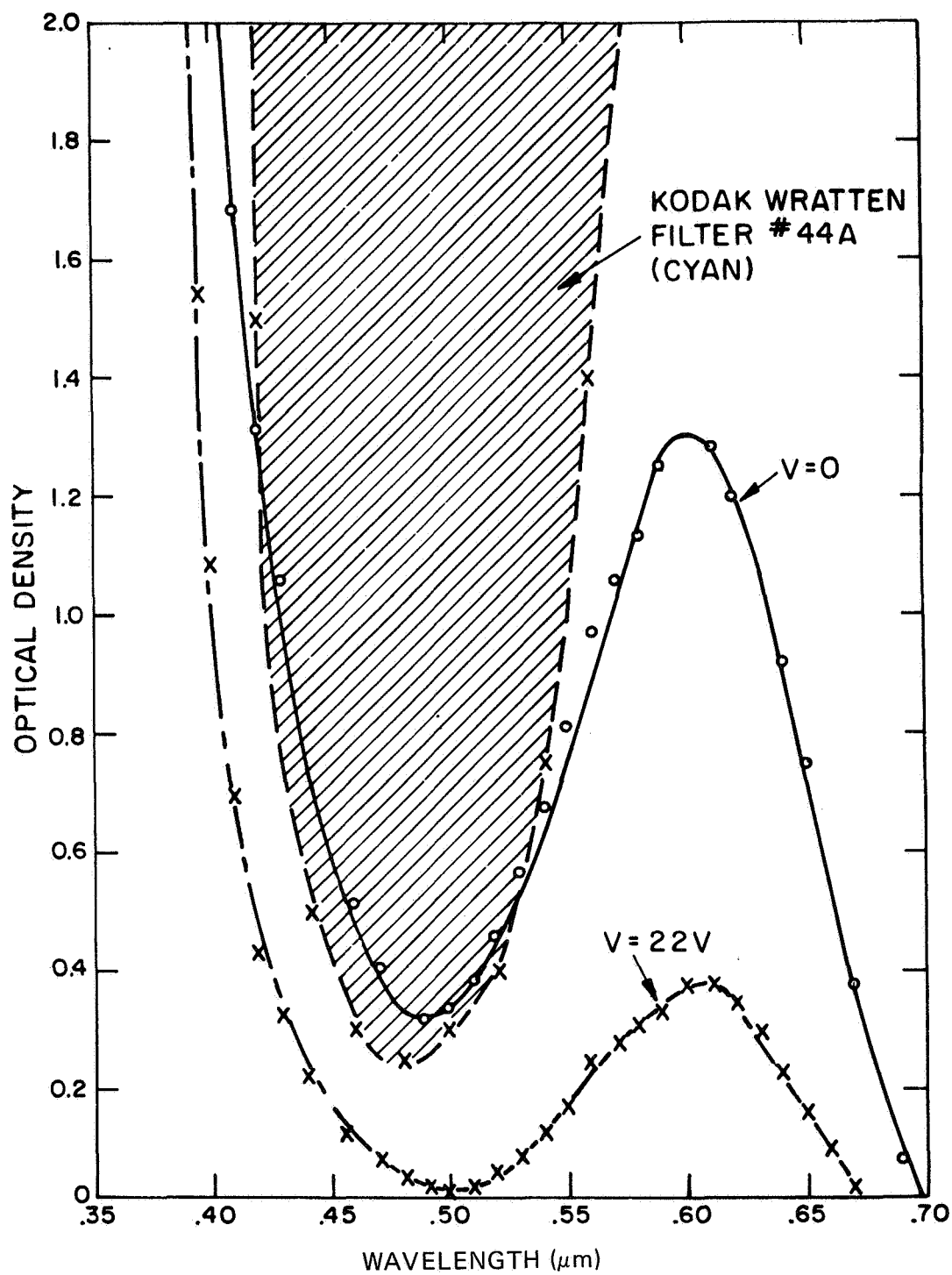


Figure 2. Optical absorption spectrum of mixture of indophenol blue and PNAZA in PEBAB-RT.



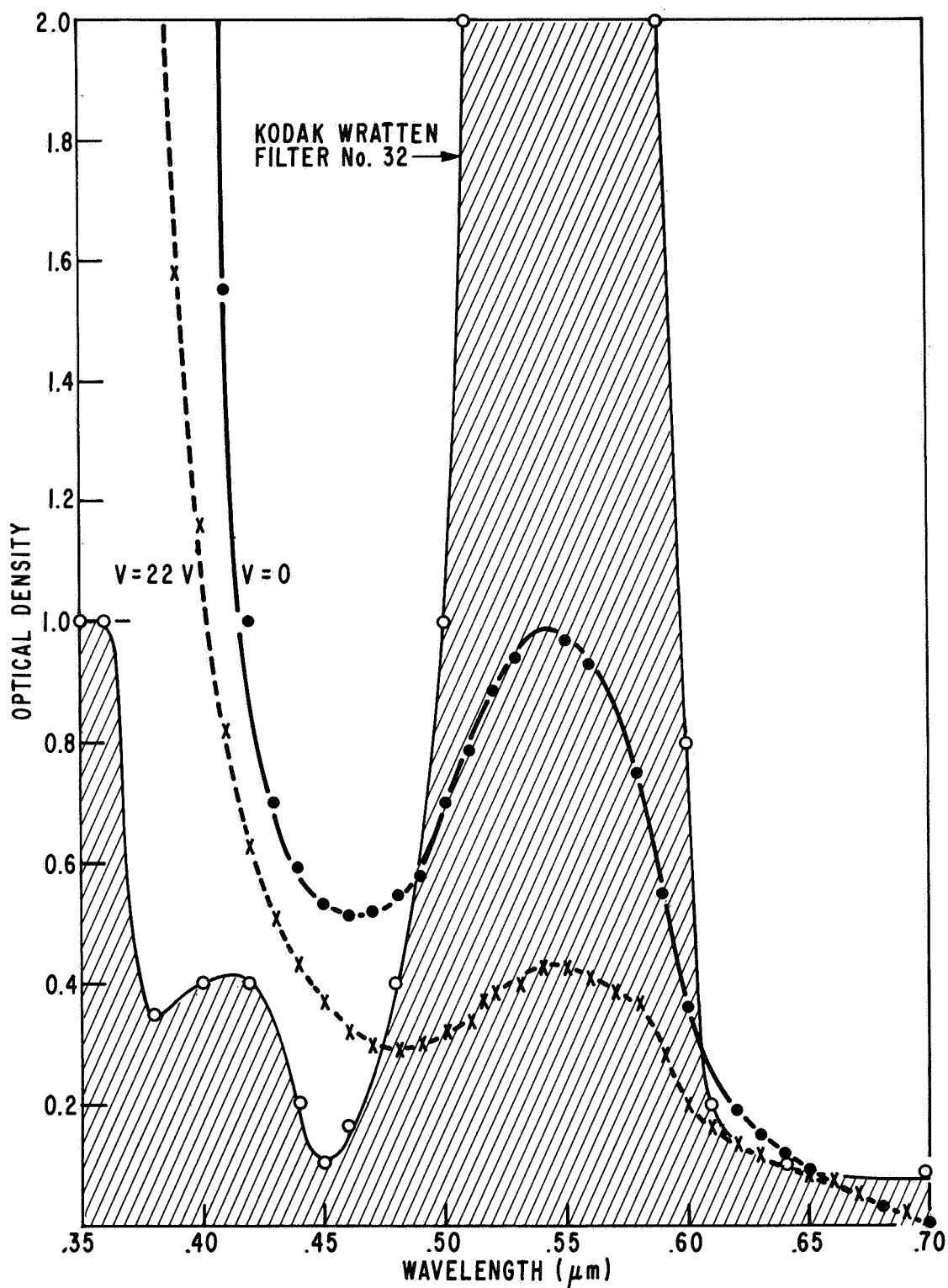


Figure 3. Optical absorption spectrum of magenta dye in PEBAB-RT.

2. Material and Device Properties — In the three-layer polychromic filter, the percentage of light absorption of each individual layer determines the hue and brightness characteristics of the composite array. Other than electronic means, adjustments in light transmission of each color layer can be made by a variation of dye concentration or by a change in cell thickness. Early in the contract period, the effects of cell thickness and dye concentration on the absorption characteristics of yellow and cyan layers were studied. Satisfactory color control was achieved using a two-layer structure consisting of:

- (a) yellow, 0.5-mil cell (1.5% dye concentration)
- (b) cyan, 0.25-mil cell (1.0% dye concentration)

These tests were made empirically to compromise the spectral content of the illuminating source ("Daylight White" fluorescent lamp) and the visual color sensitivity of the average observer.

Similar experimental tests of magenta cells have indicated that optimum color contrast occurred at  $\sim 1.0\%$  concentration of the magenta dye. Since the absorption properties of this mixture varied with thickness according to the Beer-Lambert relationship, tests were made to determine an appropriate thickness most likely to exhibit the color transmission characteristics compatible with our two-stack (cyan and yellow) device.

Unfortunately, no single thickness of the 1.0% magenta cell would allow satisfactory transmission of *both* blue and red colors when layered over this cyan-yellow combination. Variations in magenta dye concentration to improve the color saturation, hue, and brightness characteristics of the stacked array were not sufficiently effective to justify the lower color contrast ratios at dye concentrations other than the optimum of  $\sim 1.0\%$ .

In testing the three-layer stacked cell to optimize color control of the composite unit, another display problem became apparent. Using standard fabrication techniques, the three cells comprising the composite array required a total of six glass substrates. When stacked one upon another, parallax became a viewing objection. This problem is common in many liquid crystal-type devices where more than two glass surfaces are involved, but becomes more pronounced in the polychromic filter since each individual color layer exaggerates this third viewing dimension.

3. Response Time Characteristics — Frequency, field dependence, and electro-optical response measurements were made on selected magenta test cells and found to be similar to those of the cyan and yellow cells. That is, all cells have a faster rise time at higher voltages, closely following an  $E^{-2}$  field strength dependence. The relaxation time, however, remains relatively constant and independent of the magnitude of the initially applied voltage pulse ( $> 5 \times 10^3$  V/cm). Typically, a 0.5-mil-thick cell at room temperature "clears"



in about 30 ms when excited by an electric potential of 50 V (dc through audio) and relaxes back to its colored texture in about 1 to 3 sec. Anomalous transient responses common to the guest-host system have consistently complicated our efforts to accurately interpret response time data in terms of display applications. Although improved relaxation characteristics have been achieved using electronic "turn-off" methods such as gated high-frequency electric fields, these techniques require additional complex addressing circuitry.

4. Life Tests — Extended life tests of some prototype color cells have exposed a serious problem affecting the operation of the complete stacked array. Despite being sealed, the absorption spectrum of the magenta stack changed radically over a period of about 4 weeks and exhibited a brown color instead of the original magenta. Further, the current supply of magenta mixtures, carefully stored in a temperature-controlled refrigerator, has similarly changed the color absorption characteristics. No significant changes in resistivity or electro-optic response behavior could be associated with this drastic color change.

It should be noted that both the cyan and yellow portions of the color stack, fabricated very early in the contract program, have retained their original electro-optic and color characteristics. Device fabrication techniques for all three cells were essentially the same. Similarly, the same nematic host material (PEBAB-RT) was used in synthesizing all of the color mixtures and has not shown any deleterious changes over long periods of time.

The synthesis of a new batch of magenta dye has been completed for use in the fabrication of a separate magenta color cell. Improved sealing techniques and structural modifications (*vide supra*) are hopefully expected to prolong the useful lifetime of this particular mixture.

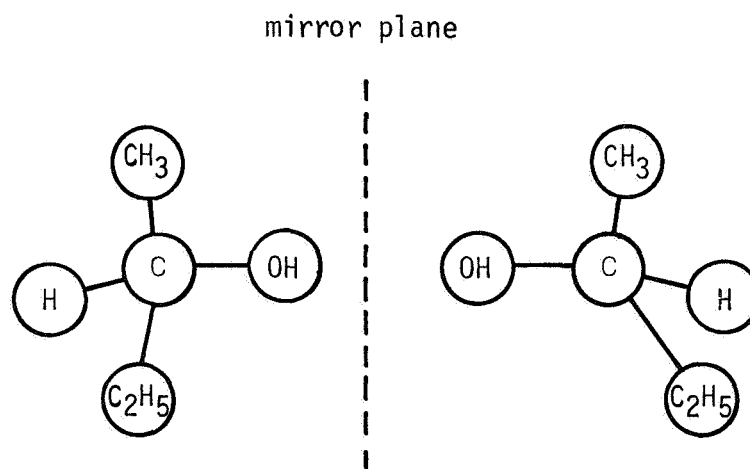
### III. FIELD-INDUCED PHASE CHANGES

#### A. Materials

It is now known that the addition of asymmetric molecules (molecules that have two mirror image forms and are said to possess chirality or handedness because they rotate a plane of polarized light in a left or right direction) to nematic liquid crystals produces the "cholesteric" mesophase. Although the mechanism of this process is yet to be determined, it appears that somehow the asymmetric center of the chiral molecule forces the nematic-type molecules into the helical conformation which characterizes the cholesteric structure. In the initial studies of field-induced phase changes (Ref. 3)

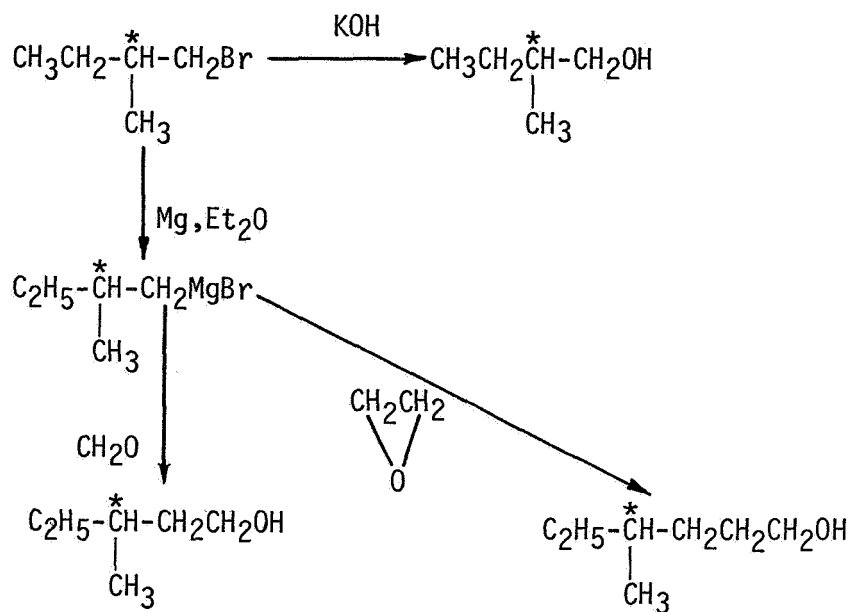
conventional steroidal-type cholesteric materials were employed. These materials required rather high fields ( $\approx 10^5$  V/cm) to effect conversion from the reflective, cholesteric state to the clear, oriented nematic phase. Our efforts, on the other hand, have been directed toward the use of nonsteroidal compounds (which are also "cholesteric") in nematic solvents. Since these molecules are generally smaller than the steroidal-type molecules, we hoped to achieve phase conversion at lower fields and higher speeds than previously observed.

The nonsteroidal cholesteric compounds have structures that are nearly identical to those of nematic compounds but with one important exception: They possess an asymmetrically substituted carbon atom, which is a carbon atom bonded to four different atoms or groups. If a molecule has such an asymmetric center, the molecule will be nonidentical with its mirror image and will therefore be optically active. However, the chemical and physical properties of each form are identical. A simple example is shown below:

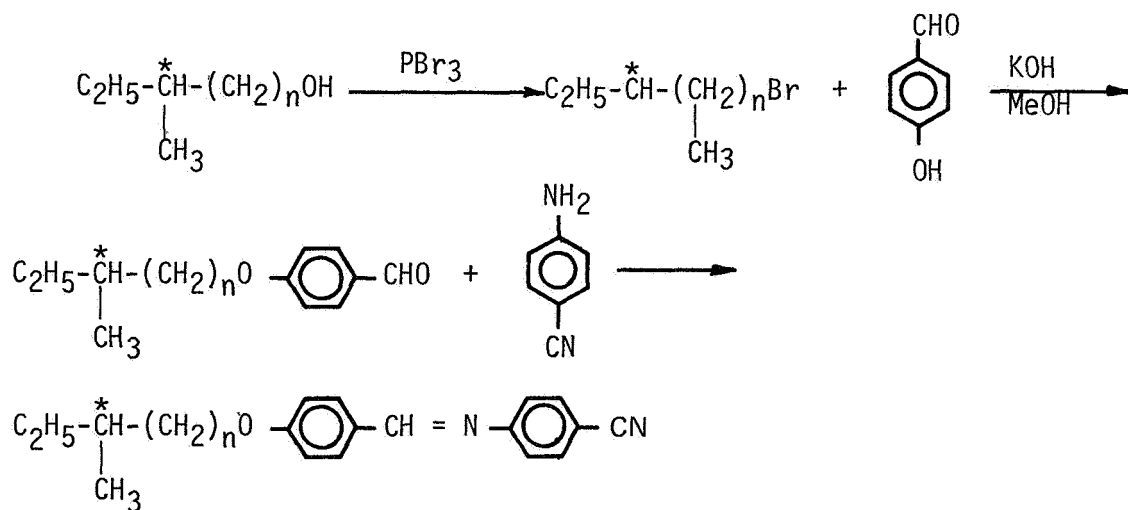


Mirror image forms of the same compound (or enantiomers), such as those shown above, are usually obtained in a mixture of equal numbers of molecules of each form. Separation of the two forms from the mixture (called a *racemic* mixture) is a tedious and time-consuming process known as *resolution*.

To avoid the problems associated with resolution, we therefore decided to prepare a series of nonsteroidal compounds from optically active starting materials. This was accomplished by the following sequence of reactions:

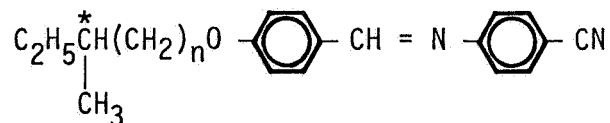


Each of these alcohols was then used to prepare the Schiff base compounds as follows:



The transition temperatures for this series of compounds are listed in Table I, and a plot of these values vs. the number of carbon atoms in the methylene chain is illustrated in Figure 4. Note that as the chain length is increased, the smectic thermal stability rises at the expense of cholesteric thermal stability until the compound with  $n = 5$  shows smectic behavior exclusively. This is identical to the results obtained with

TABLE I  
Optically Active p-Alkoxybenzylidene-p'-Aminobenzonitriles<sup>a</sup> \*



n	Transition Temperatures, °C <sup>b</sup>		
	Crystal-Smectic	Smectic-Cholesteric	Chol-Isotropic
1	—	—	57 (39) <sup>c</sup>
2	—	—	63 (50) <sup>c</sup>
(CH-1) 3	40	48	66
4	55	59	66.5
5	34	—	77 <sup>d</sup>
a) Satisfactory analysis was obtained for each compound. b) Transition temperatures were determined with a Thomas-Hoover melting point apparatus and a DuPont Model 900 Thermal Analyzer with DSC cell. The textures of the mesophases were examined with a Bausch and Lomb polarizing microscope equipped with a hot stage. c) Monotropic. d) Smectic-Isotropic Transition.			

compounds that possess both smectic and nematic behavior (Ref. 6). The increased chain length produces a separation of the primary dipolar groups and thus reduces the terminal to lateral cohesive forces. This increase in lateral cohesions then gives rise to increased smectic thermal stability.

It was possible to drastically reduce smectic thermal stability and to broaden the cholesteric temperature range by making mixtures with nematic host compounds. Since the compound with  $n = 3$  (designated CH-1) had the broadest temperature range, it was chosen as the guest molecule in mixtures with PEBAB-RT.

---

\*The general series was proposed and certain of its members synthesized in the laboratory prior to receiving the present contract. During the contract period, additional new members of the series were synthesized for the first time.



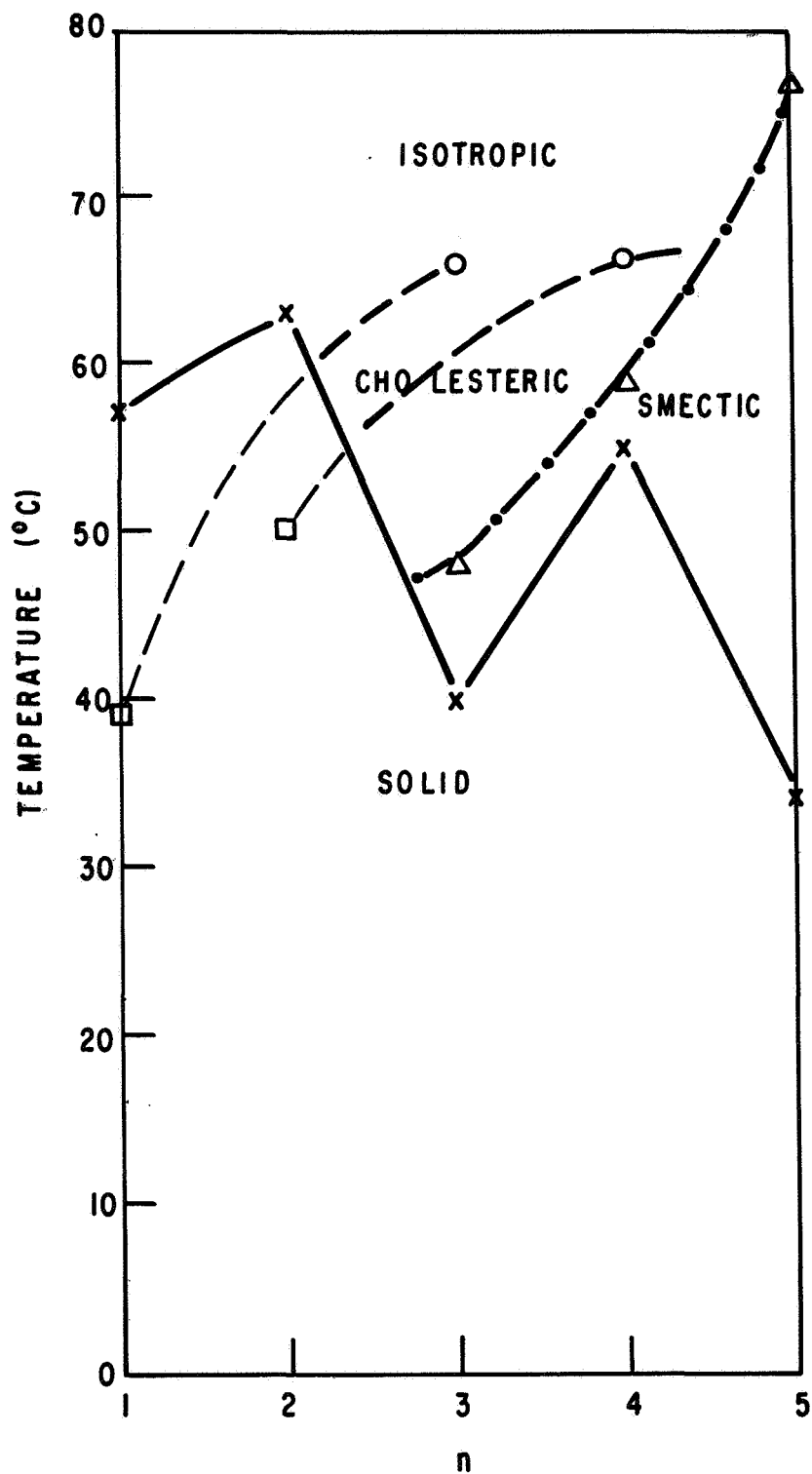


Figure 4. Phase transition plot of series:  
 $C_2H_5CH(CH_3)(CH_2)_nOC_6H_4CHNC_6H_4CN$ .

A phase diagram illustrating these results is presented in Figure 5. Note that the smectic-cholesteric transition decreases sharply with decreasing concentrations of the optically active component, and at concentrations below  $\sim 80\%$  the material exhibits only the cholesteric mesophase. All of the mixtures tended to supercool far below their "theoretical" crystal-mesomorphic transition temperatures, and thus accurate melting point determinations could not be obtained for most of the mixtures (the presence of a glassy state was noted in these mixtures at low temperatures). The "theoretical" crystal-mesomorphic transitions shown in Figure 5 were calculated from the standard cryoscopic equation which is

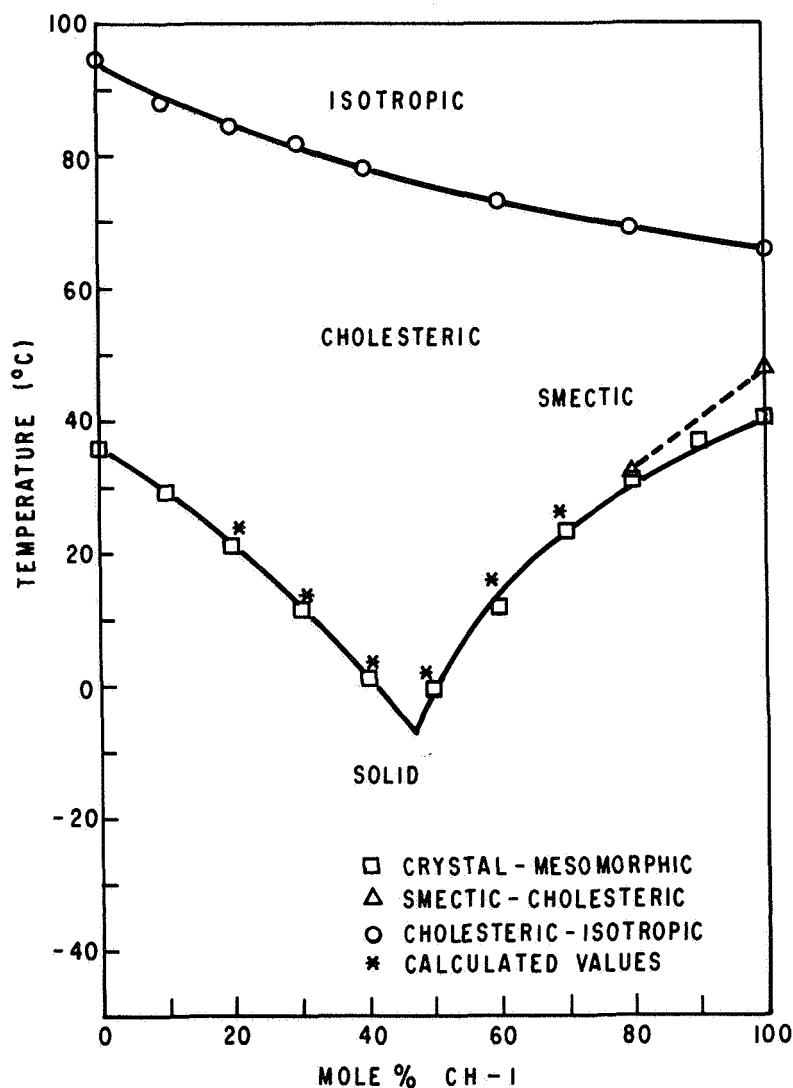


Figure 5. Phase diagram of binary mixture of CH-1 in PEBAB-RT.

derived from the Clausius-Clapeyron equation. This derivation is based on a number of assumptions and would not be expected to hold except at low concentrations (ideal dilute solutions) of one component (solute) in the other (solvent). The equation is given by:

$$\frac{d \ln x}{dT} = \frac{L_f}{RT^2} \quad (\text{modified van't Hoff equation})$$

where  $x$  is the mole fraction of the "solvent,"  $L_f$  is the molar heat of fusion (assuming that Raoult's law is applicable) and  $R = 1.9869 \text{ cal/}^\circ \text{ mole}$ . When  $x$  is unity (pure "solvent") the melting point is  $T_0$  and integration between  $T$  and  $T_0$  (assuming  $L_f$  to remain constant) gives:

$$\ln x = -\frac{L_f}{R} \left( \frac{1}{T} - \frac{1}{T_0} \right)$$

or

$$T = -\frac{T_0}{1 - \frac{RT_0}{L_f} \ln x}$$

where  $T$  is the calculated melting point of the mixture.

Although this is a crude approximation, we have found it possible to determine the composition of the eutectic mixture using this calculation. The experimental value of the melting points of any particular eutectic mixture, however, generally differs from that predicted by the modified van't Hoff equation. This is to be expected since these mixtures are not ideal, dilute solutions. The significant result here is that smectic mesomorphism gives way exclusively to cholesteric mesomorphism by the addition of nematic compounds.

All of the compounds of Table I have a nitrite group ( $C \equiv N$ ) in the terminal position of the molecule. This provides the molecule with a high dipole moment along the molecular axis and consequently with positive dielectric anisotropy, a property which is essential to our electro-optic measurement program. Evaluation of these materials is presented below.

## B. Electro-Optic Behavior

Another electro-optic effect which employs a guest-host type of interaction is that obtained by the field-induced change of a cholesteric to a nematic mesophase. Appropriate

mixtures of cholesteric and nematic liquid crystals can be considered as merely an extension of the guest-host systems described previously. Instead of a corresponding color change, however, modification of the lattice structure (or phase) of the cholesteric component by application of a sufficiently large electric field is optically detectable as a change from a scattering to a homeotropic texture.

Field-induced changes from the cholesteric to the nematic mesophase involve the unwinding of the characteristic helical structure followed by an orientation of domains. This results in a change from a reflective state to a clear state. Studies of the mechanism of this effect were conducted through detailed measurements of material properties and response characteristics to determine first-order effects of structural variations on device electro-optical performance.

Early studies had indicated that the magnitude of the electric field required to produce field-induced phase changes was in the order of  $\sim 1.5 \times 10^5$  V/cm. The synthesis of several new nonsteroidal cholesteric compounds has led to the development of mixtures which require lower operating voltages and operate at higher speeds.

No consistent relationship between material composition and device resistivity could be accurately determined above a minimum value of  $\sim 10^9$  ohm-cm.

1. Field Dependence — A detailed investigation of the field dependence and light-scattering characteristics of the nonsteroidal cholesteric materials was made during the contract period. The experimental setup is shown at the top of Figure 6. For these particular measurements, the incident light was directed normal to the cell surface and detected through crossed polarizers with a photomultiplier located on-axis with the incident light beam. A plot of relative brightness versus applied voltage (60 Hz) for various concentrations of CH-1 in PEBAB-RT is also shown in Figure 6. The results shown indicate an increase in scattering with increasing concentrations of CH-1 (no field applied). Cell brightness decreases sharply with increasing voltage but the relationship between concentration and the field required to render the cell "clear" (relative brightness = 0) is not clear-cut. Note that for excitation voltages between 30 and 40 V, contrast ratios of greater than 100:1 can be achieved. Previously reported steroidal cholesterics have required over 100 V to produce contrast ratios of 10:1. These results show that the voltages required to produce the change from the planar texture of the cholesteric mesophase to the homeotropic texture of the nematic mesophase are considerably lower for the nonsteroidal cholesterics.

The peaks which appear in the brightness-voltage curves are believed to be due to the chromatic behavior of the birefringence. That is, the light transmitted through the cell may be of varying wavelength as the helical pitch changes. Alternatively, these peaks may be due to a reordering of helical domains which precedes helix unwinding.

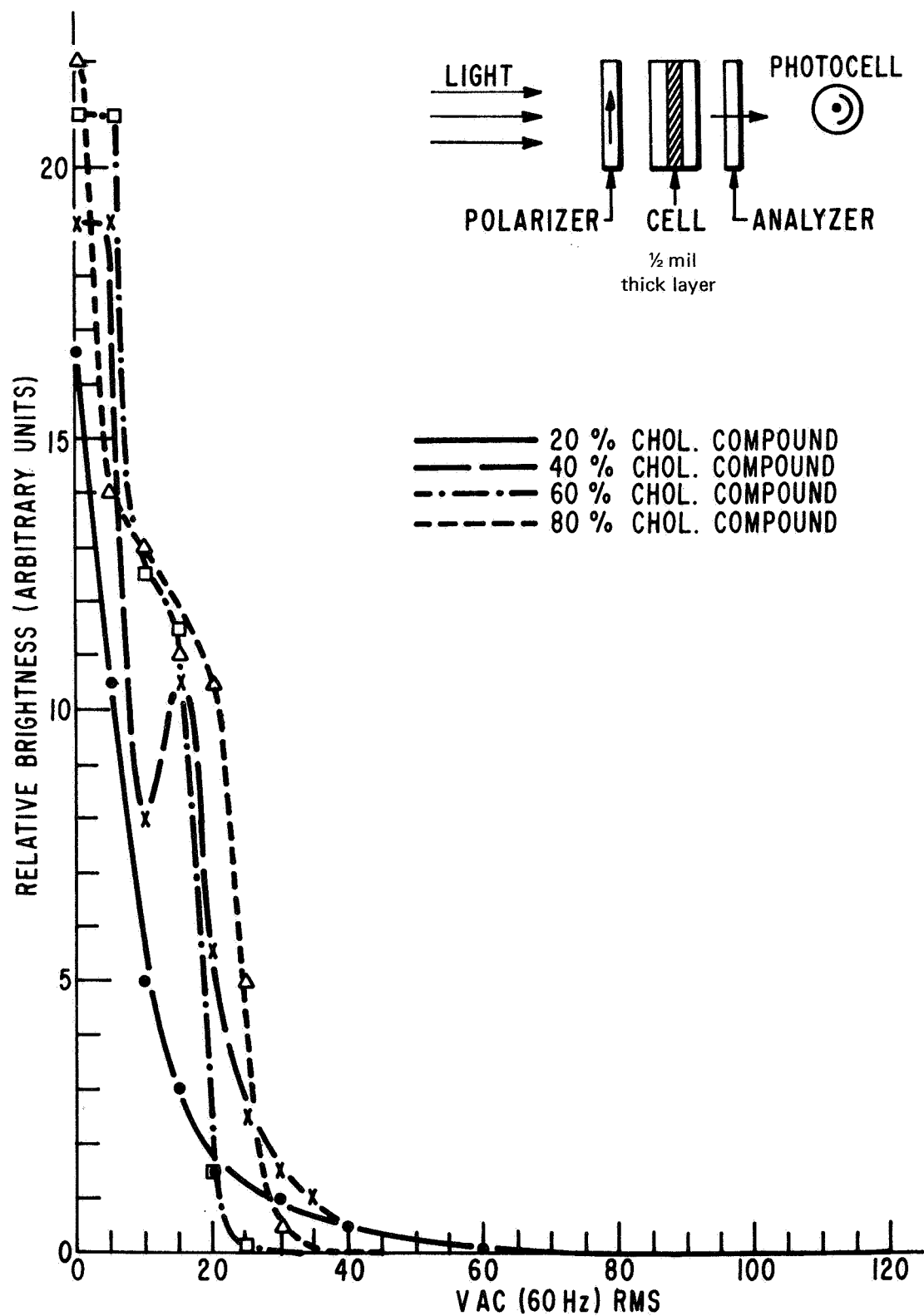


Figure 6. Relative brightness vs. voltage for four different mixtures.



2. Light-Scattering Characteristics — To optimize display-related parameters, a series of measurements were made to gain a better understanding of the light-scattering properties characteristic of field-induced phase changes. The experimental arrangement for measuring the scattering parameters and the angular notations used in these measurements is shown in Figure 7. The light source is a microscope lamp, collimated so that the light incident on the cell has an angular spread of about 5 degrees. Both the angle of incidence ( $\theta$ ) and the angle of measurement ( $\phi$ ) could be varied but light propagating outside the plane of the diagram was not considered.

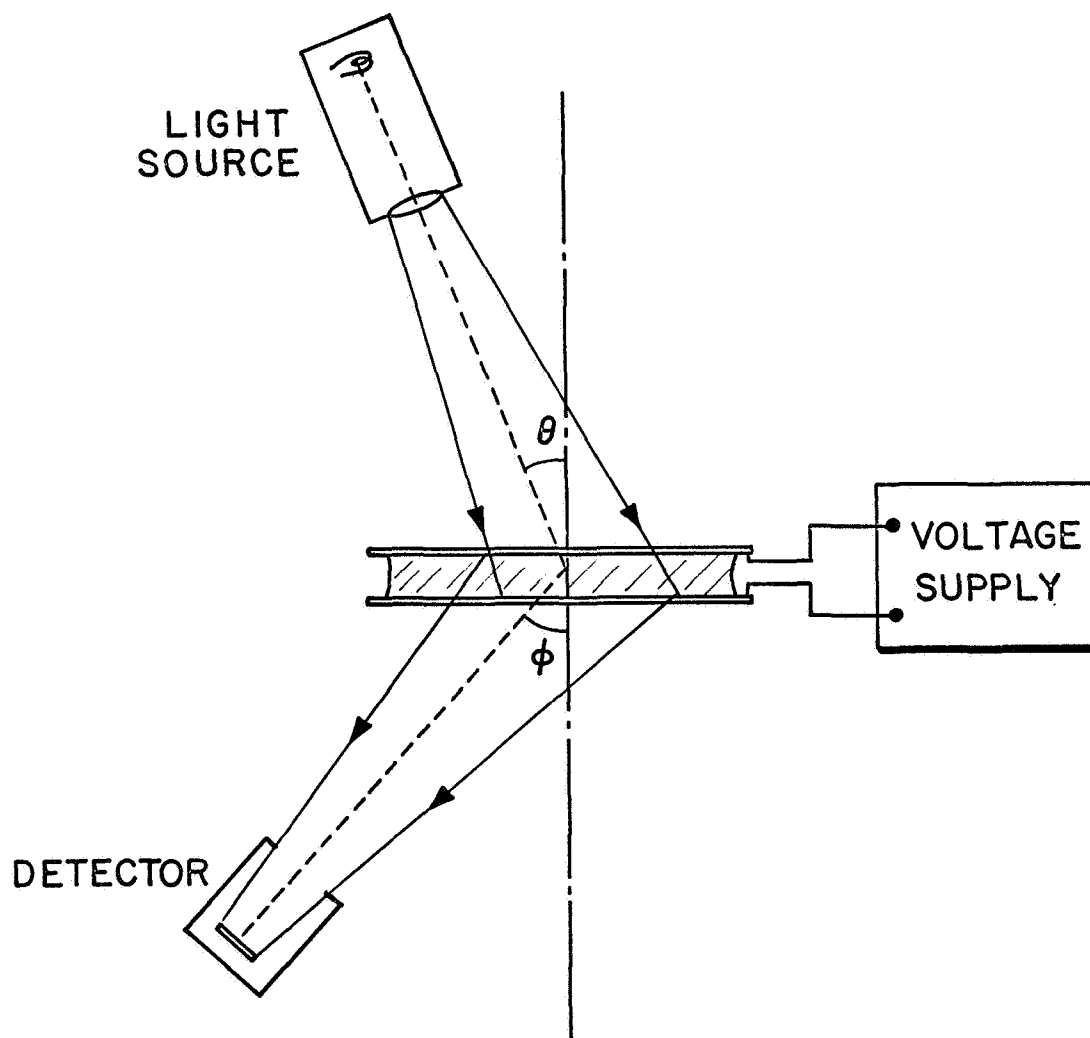


Figure 7. Experimental arrangement for measuring light scattering of liquid crystal cells.

The scattered light was measured in two different ways. In one method, no polarizers were used and the scattered light was measured with a photomultiplier. A typical graph of light scattering as a function of detector angle for a 0.5-mil cell containing  $\sim 40\%$  CH-1 in PEBAB-RT is shown in Figure 8. From this curve it can be seen that maximum contrast is restricted to a narrow viewing angle of  $\sim 5$  to  $15^\circ$  removed from the incident light source. Similar results were obtained with the detector angle fixed at  $0^\circ$  and the angle of incidence varied between  $-10$  and  $+45^\circ$ . Without the use of crossed polarizers, maximum brightness occurs in both the scattering and clear states when the light source and detector are "on axis" ( $\theta = -\phi$ ). Within a few angular degrees of this specific condition, a polarity reversal of the contrast ratio exists; i.e., the light reaching the detector is greater when the liquid crystal cell is "clear" than in its scattering texture.

In the second measurement technique, crossed polarizers were introduced between the light source and photodetector (as illustrated in Figure 6) and the light intensity was measured with a spot brightness meter. This was a condition that a viewer would likely observe in an actual display.

Since optimum display performance may not necessarily be restricted to the geometrical arrangement with the incidence angle ( $\theta$ ) or detector angle ( $\phi$ ) normal to the cell surface, further light-scattering measurements were made by variation of both the incidence and scattering directions. The contrast ratio of a standard test cell containing 40% CH-1 in PEBAB-RT at four different incidence angles ( $\theta$ ) is shown in Figure 9. A similar plot for a 60% CH-1 mixture is compared in Figure 10. At incidence angles much greater than  $20^\circ$ , the contrast ratio decreases sharply for both mixtures. Since the light scattered in the "clear" state ( $V = 50$  volts) appears to be mainly dependent on the relative scattering angle from input to output ( $\theta + \phi$ ) this decrease in contrast appears to be primarily due to an intensity reduction of the scattering texture ( $V = 0$ ) at high angles of incidence.

To compare device performance using crossed polarizers in the measurement apparatus, a number of similar tests were made with materials of different compositions. In most cases, a contrast enhancement by an order of magnitude was readily achieved. The contrast improvement of a 40% CH-1 mixture at various angles of incidence (detector angle  $\phi$  fixed at  $0^\circ$ ) is shown in Figure 11. Even at large displacement values between the incidence and scattering angles, a contrast ratio greater than 20:1 was calculated. However, one of the possible objectionable display features using crossed polarizers that is not evident in the light-scattering or contrast ratio measurements are the color changes discernible at certain viewing angles. Instead of the usual white-to-black contrast change, practically any of the colors in the visible spectrum can be observed at specific scattering angles. This results in the contrast occurring from color-to-black. This was observed, to some degree, with all of the mixtures evaluated. It should be mentioned here that the introduction

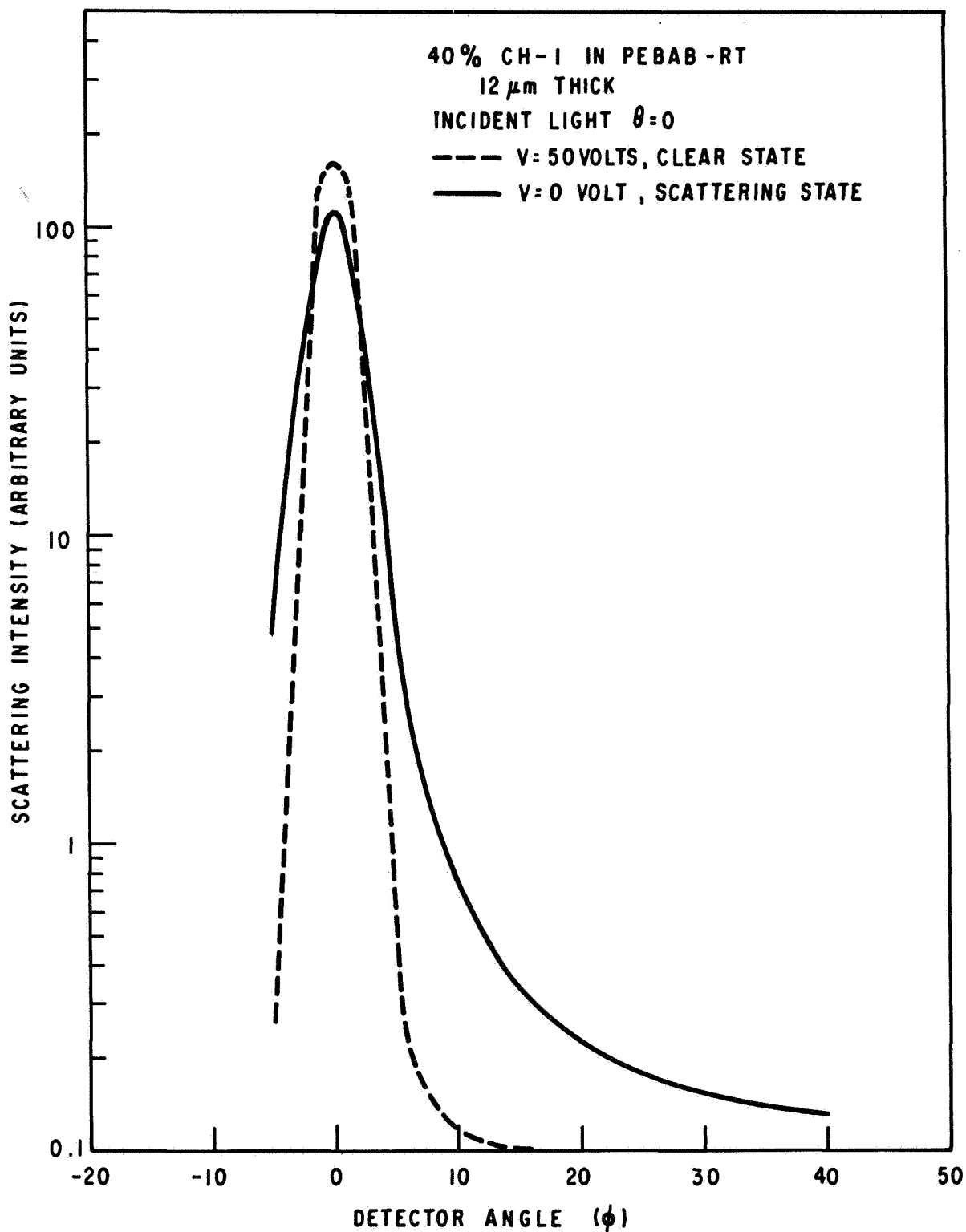


Figure 8. Scattering intensity vs. detector angle.

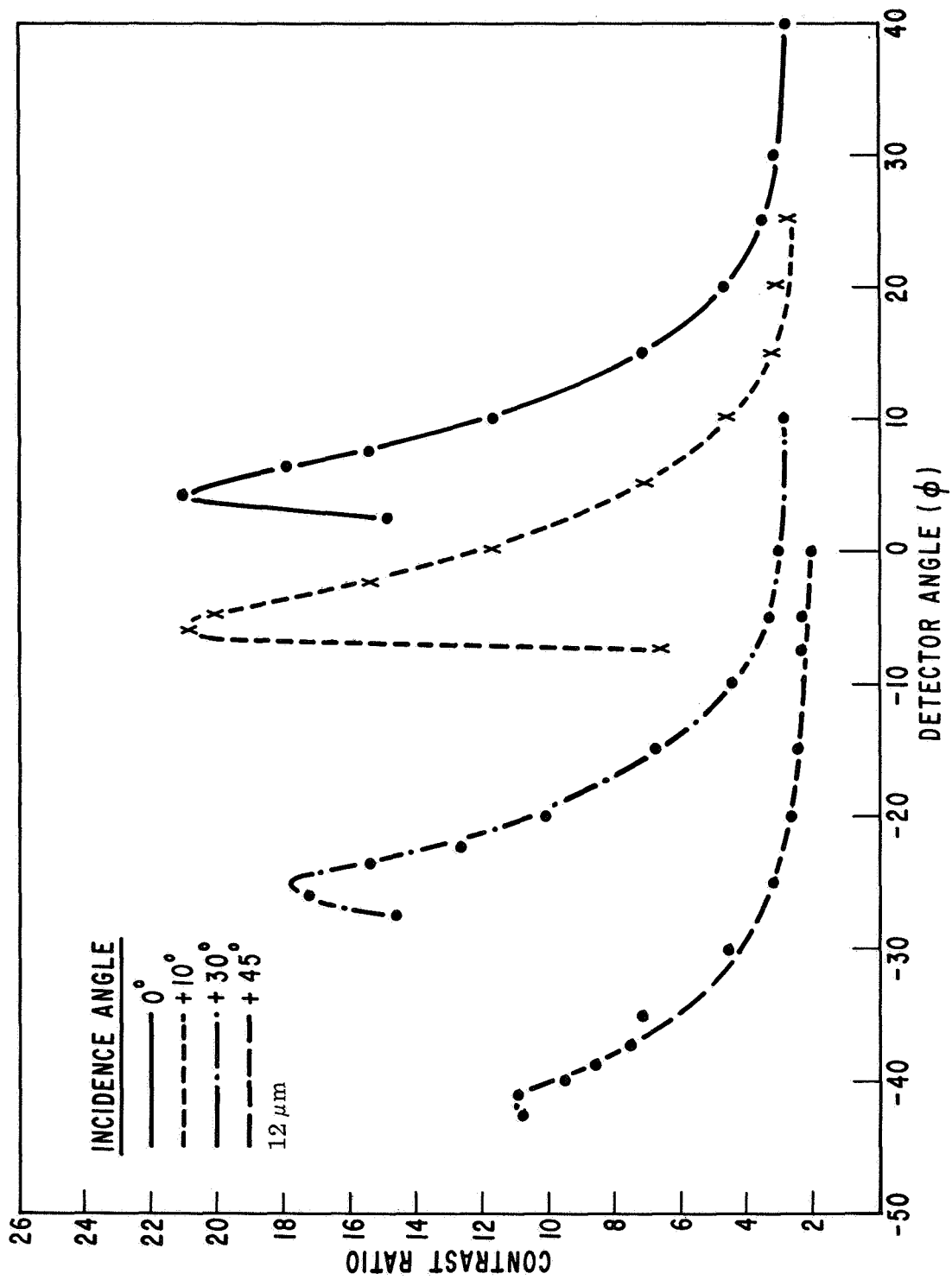


Figure 9. Angular dependence of contrast ratio as a function of incidence angle, (40% CH-1 mixture).

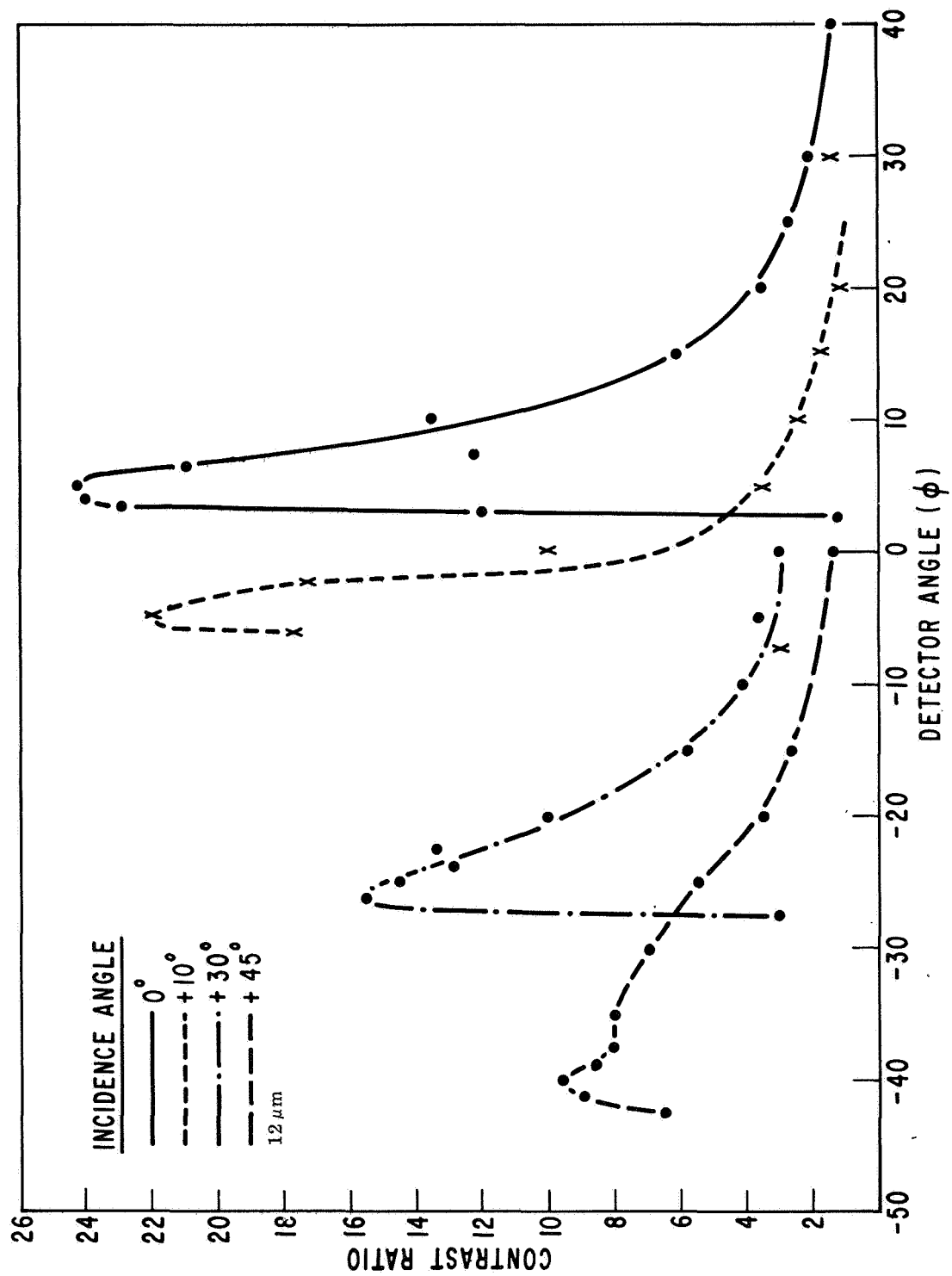


Figure 10. Angular dependence of contrast ratio as a function of incidence angle, (60% CH-1 mixture).



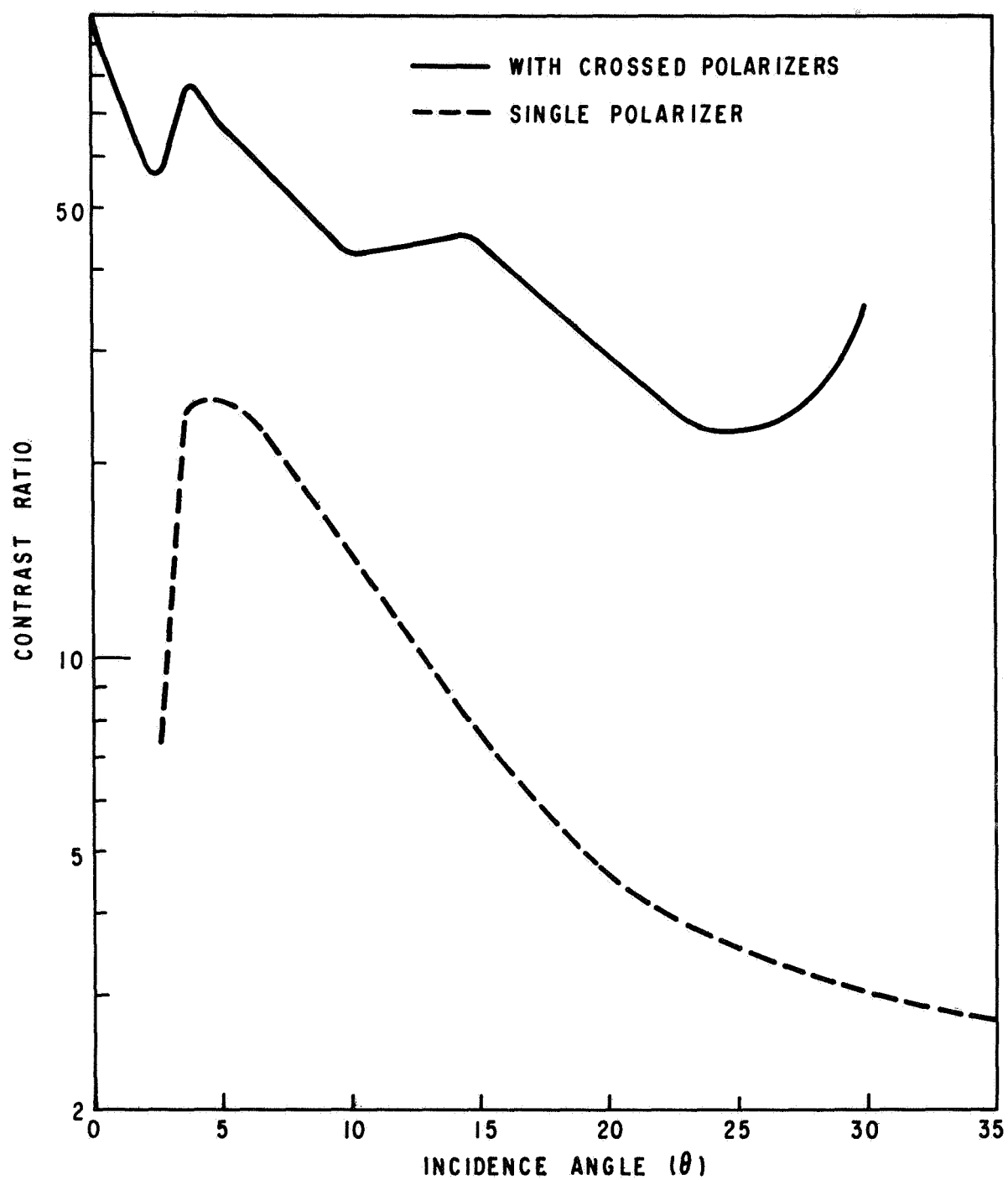


Figure 11. Contrast improvement using crossed polarizers. 40% CH-1,  $\frac{1}{2}$  mil cell, detector angle =  $0^\circ$ .

of even small amounts of CH-1 into the host nematic material will render the entire mixture cholesteric. The pitch of the helix in the cholesteric structure, however, is determined by the concentration of the optically active component and hence the color of the transmitted light at any particular scattering angle.

The results of these measurements offered some means of comparing various cholesteric-nematic mixtures and of optimizing display characteristics. For instance, only slight differences in scattered-light intensity were noted for cholesteric compositions within the 20% to 60% range. Since the absolute value of scattered-light intensity determines brightness and contrast ratio, material composition could be chosen to optimize other device properties such as temperature range and speed of response. Significant contrast enhancement was also observed when crossed polarizers comprised part of the optical system. This feature may be especially useful when color changes at various viewing angles are not objectionable.

3. Response Time Characteristics — Measurements of electro-optic response were made for materials in the composition range of 5% to 80% CH-1 in PEBAB-RT. The response and relaxation behavior of these mixtures exhibited complex two-step processes. These results suggest that helical unwinding is preceded by a reorientation of the helices.

The response time as a function of dc voltage for some of these mixtures is shown in Figures 12 and 13. In Figure 14 the electro-optic response as a function of applied ac voltage for similar mixtures is compared. At increasing voltages, the response time decreases sharply and appears to fit the relationship  $\tau \sim \exp E^{-2}$  (Ref. 2) only at higher voltages.

A detailed examination of the response properties of test cells exhibiting the field-induced phase change has revealed some anomalous characteristics that may be relevant to the mechanism involved in the unwinding process of the helical structure. Distinct peaks in the brightness versus voltage curves generally appear at some value just slightly less than that voltage required to “clear” the test cell to its minimum value. As viewed through crossed polarizers, the clear texture results in little or no light transmitted to the photodetector. With no polarizers present, this same condition would represent maximum light transmission or brightness. For most experimental purposes, the use of crossed polarizers in the light detection system has provided a readily discernible means of observing subtle variations in surface texture.

Similar brightness peaks are also evident and even more pronounced in the relaxation characteristics when the excitation field has been removed. Although all of the various mixtures exhibited this anomalous relaxation behavior to some degree, electro-optic measurements revealed these “transients” to be also dependent on the repetition rate,

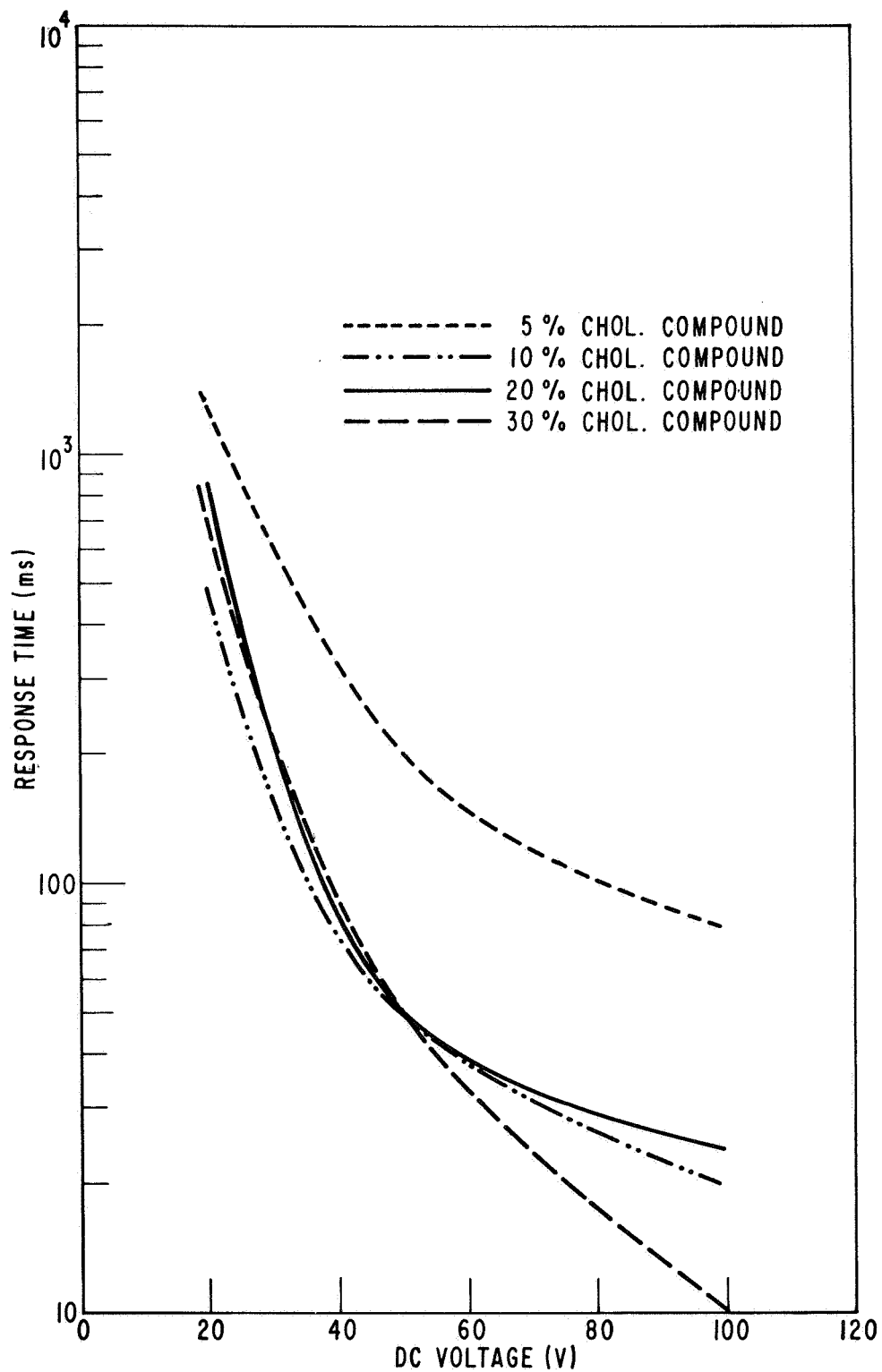


Figure 12. Response time (dc) as observed with crossed polarizers.

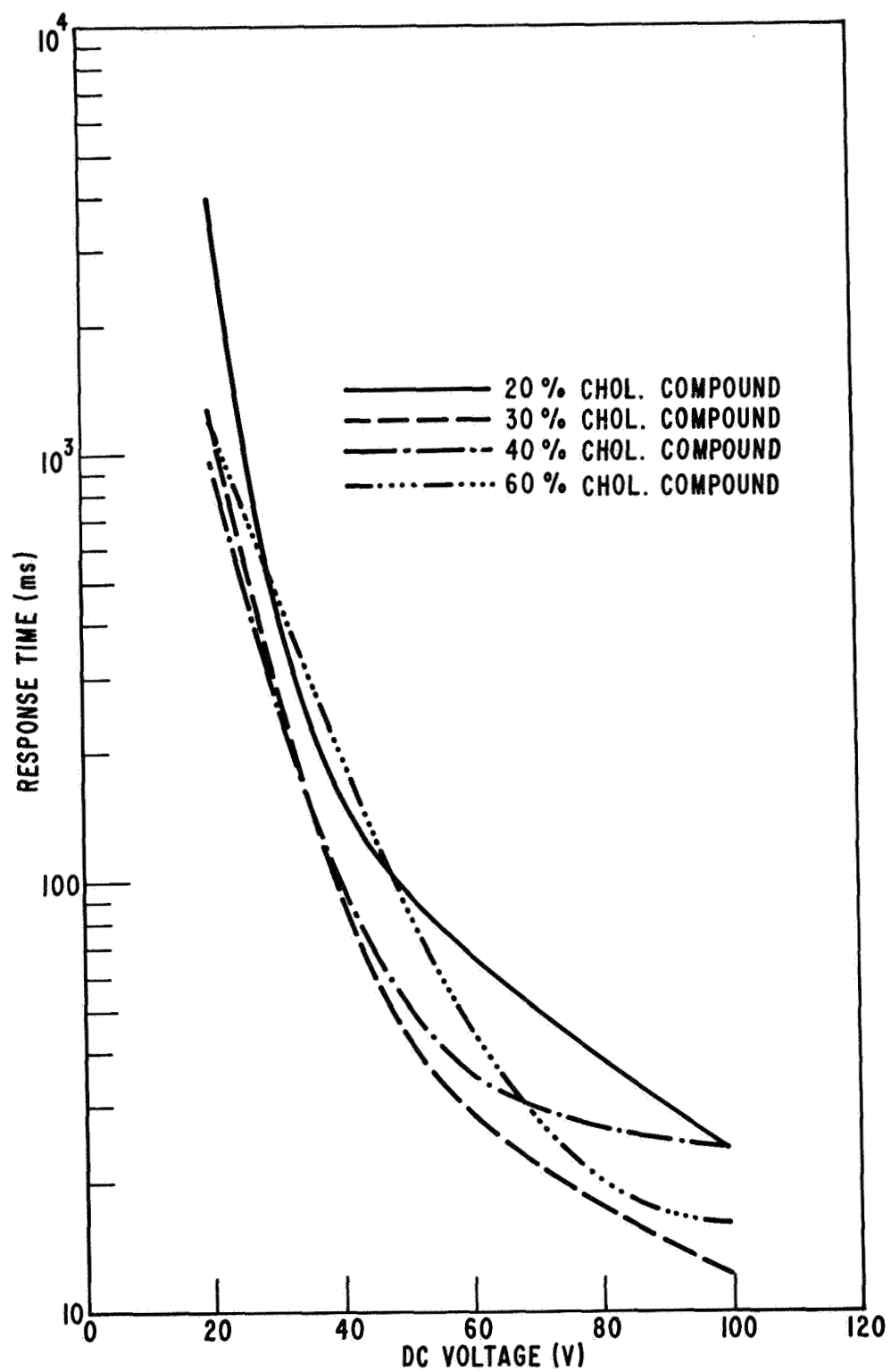


Figure 13. Response time (dc) as observed with crossed polarizers.

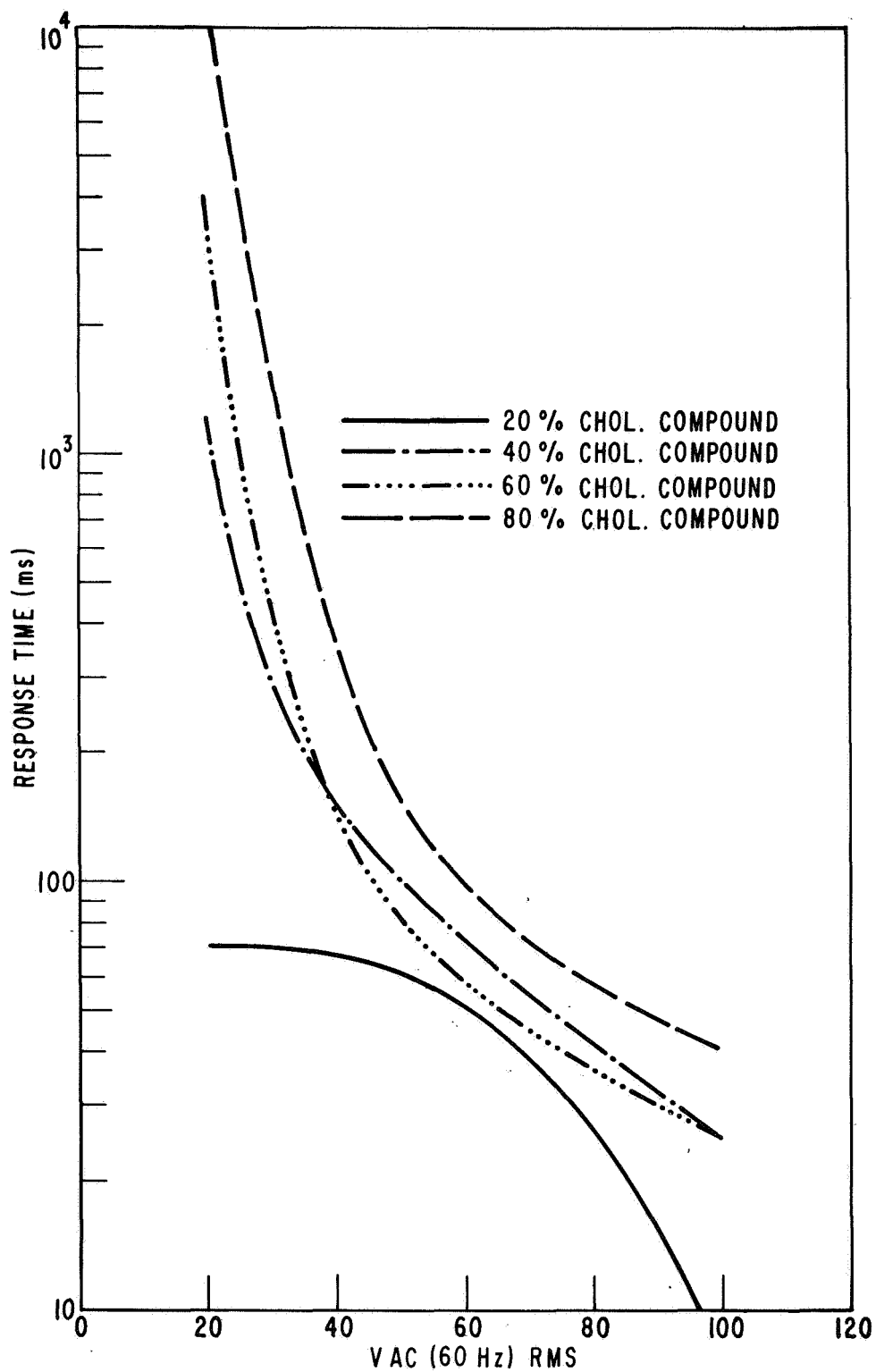


Figure 14. AC response time as observed with crossed polarizers.



pulse width, and magnitude of the originally applied dc voltage. It should be mentioned here that very similar response anomalies have been reported earlier (Ref. 2) in measurements of our color mixtures using the same PEBAB-RT host material. The most immediate problem presented by this behavior is that it complicates our efforts to accurately interpret response time data. There appear to be at least two different relaxation processes that occur after removal of the excitation field. A typical relaxation curve (using crossed polarizers) of brightness versus elapsed time is shown in the photograph of Figure 15. Note the rapid increase in brightness to a maximum value in less than 100 msec followed by another exponential-type increase requiring about 1 second to attain ~ 90% of its steady-state value.

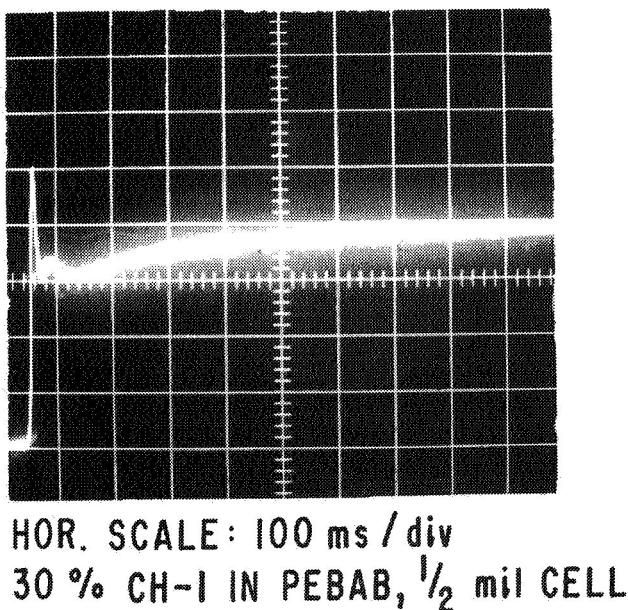


Figure 15. Two-step electro-optic relaxation characteristic.

The relaxation data presented in Figure 16 do not include the long time exponential-type decay process which was found to be dependent on the initially applied voltage pulse. The initial rapid decay process, however, appeared to remain relatively constant and independent of the original addressing conditions. At room temperature, the relaxation time increases as a function of increasing concentration of CH-1 (20-60%), which is in good agreement with the linear relationship described by Heilmeier, et al. (Ref. 4).

Based on these experimental observations, it is indeed possible that the reorientation process is composed of a two-step mechanism. One possible interpretation of the relaxation

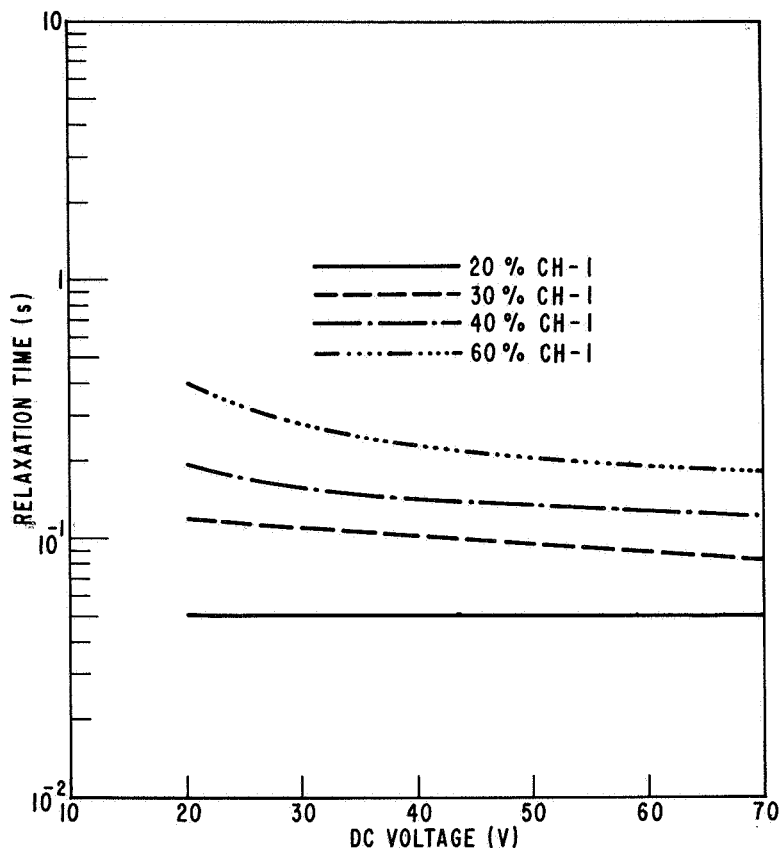


Figure 16. Relaxation time as observed with crossed polarizers,  $\frac{1}{2}$  mil cells, incidence angle =  $0^\circ$ , detector angle =  $0^\circ$ .

characteristics is a reordering of the helical domains prior to the winding of the helix structure. A second possibility is a rapid molecular realignment within the bulk material and a much slower reorientation process dictated by wall (surface) forces of the constraining glass electrodes.

In addition to these two relatively rapid relaxation processes, there is another process that occurs over a much longer period of time. When the cell relaxes from its clear state ( $\sim 1$  sec), it forms a highly scattering state which changes slowly ( $\sim 15$  to  $20$  minutes) to the stable, planar texture. This highly scattering state is thought to consist of helical domains which have their axes oriented at many angles immediately after the field is removed. This metastable condition is short-lived when no field is applied but under the influence of a very low strength field ( $\sim 2$  to  $3$  V) this texture can be observed indefinitely.

4. Device Thickness — In order to optimize the design of a display device and to further develop a model of the field-induced structure change, the thickness dependence of various electro-optical parameters was measured. The intensity and angular dependence of the scattered light for four different cells (40% CH-1 in PEBAB) ranging in thickness between 6 and 50  $\mu\text{m}$  varied only slightly. Apparently, the scattering medium is not a uniform one since it would be expected that the thickness dependence would result in an exponential-type attenuation of the scattered light beam.

One possible explanation for this effect is that most of the light scattering occurs at or near the glass electrode liquid crystal interfaces which have the same properties regardless of the thickness of the cell. To support this possibility very little variation in electro-optic relaxation time as a function of cell thickness was experimentally noted. Also, the thinnest cells (6  $\mu\text{m}$ ) were not as stable as the thicker cells; i.e., the amount of light scattering decreased with time after the excitation field had been removed. There was a partial reversion to the clear state which reached saturation in about 45 minutes. These observations are compatible with the possibility that many of the structural variations occur near the cell surface and these wall forces can have a large dominating influence on electro-optical performance.

5. Temperature Effects — Measurements of response and relaxation behavior of a 40% mixture of CH-1 in PEBAB-RT as a function of temperature were made during the contract period. A 12.5- $\mu\text{m}$  layer of the liquid crystal was used and both the response and relaxation time decreased with increasing temperature. For example, at 30 V the response time decreased from 300 msec at room temperature to 40 msec at 55°C and 12 msec at 73°C. This response also appears to be a two-step process — each step having a separate temperature dependence. At elevated temperatures, the two-step electro-optical response process is only slightly detectable.

The relaxation time decreased from 200 msec at room temperature to 40 msec at 73°C. In this nematic range, the relaxation time followed a  $K \exp. E_0/kT$  temperature dependence. Earlier measurements (Ref. 2) have shown the temperature dependence of both the viscosity and resistivity of the host PEBAB-RT materials to be similarly proportional to  $\exp. E_0/kT$  which suggests that the relaxation process is related to the mixture composition by the square root of the viscosity.

6. Device Evaluation — Seven-segment numeric devices operated in the reflective and transmissive modes have been fabricated to provide a visual demonstration of potential device applications. In both of these devices problems were encountered in viewability. These problems appeared to be due to the technique of addressing the numeric. For example, in attempting to address the cell with the BCD decoder-driver arrangement used for dynamic scattering cells, it was impossible to obtain the maximum contrast between the activated and unactivated segments. This was due to the fact that in the unactivated

segments the material had relaxed to the weakly scattering planar texture. Introduction of crossed polarizers was found to produce enhanced contrast but this type of display would probably require a separate light source.

In addition to numerical displays, field-induced phase changes may also be useful in bar-graph and window-type displays. These types of displays are particularly suited to aircraft or spacecraft application where changes in data rather than absolute values are of primary importance. One type of bar-graph display that may find utility as an engine monitoring indicator is described in the following section.

#### IV. STATE-OF-THE-ART DEVICES

##### A. Electronically Controlled Color Filter

A two-layer polychromic filter which can be electronically tuned was constructed during the contract year. The operation of the filter is based on the cooperative alignment of pleochroic dye molecules by nematic liquid crystals activated by electric fields. This orientational effect produces changes in the optical density of the material and thus changes in the color of the light transmitted through the medium.

The device consists of two separate color cells containing pleochroic dye molecules that transmit the colors of either cyan or yellow. In combination, four different colors can be produced by electronic control of the individual cells. Ideally, a third stacked cell containing a pleochroic magenta dye would have allowed color selection over most of the visible portion of the electromagnetic spectrum.

The pleochroic dyes chosen for this device constitute the primary colors of a subtractive color system. A cyan filter transmits blue and green light but absorbs red light; hence, it subtracts the primary red from white light. Similarly, a magenta filter, which transmits blue and red, subtracts green from white light; and a yellow filter, which transmits green and red, subtracts blue from white light.

We could not use an additive system (e.g., red, blue, green) because, to a considerable extent, these filters are mutually exclusive; that is, none of them transmit the light passed by the other two. Hence, any two of the filters superimposed over the light source would cut out substantially all the light.

With a subtractive system, however, this is not the case. Since each of the filters transmits about two-thirds of the spectrum, we can superimpose them over a single light

source to produce other colors. For example, the cyan and yellow filters in combination subtract the red and blue from white light and allow green to be transmitted.

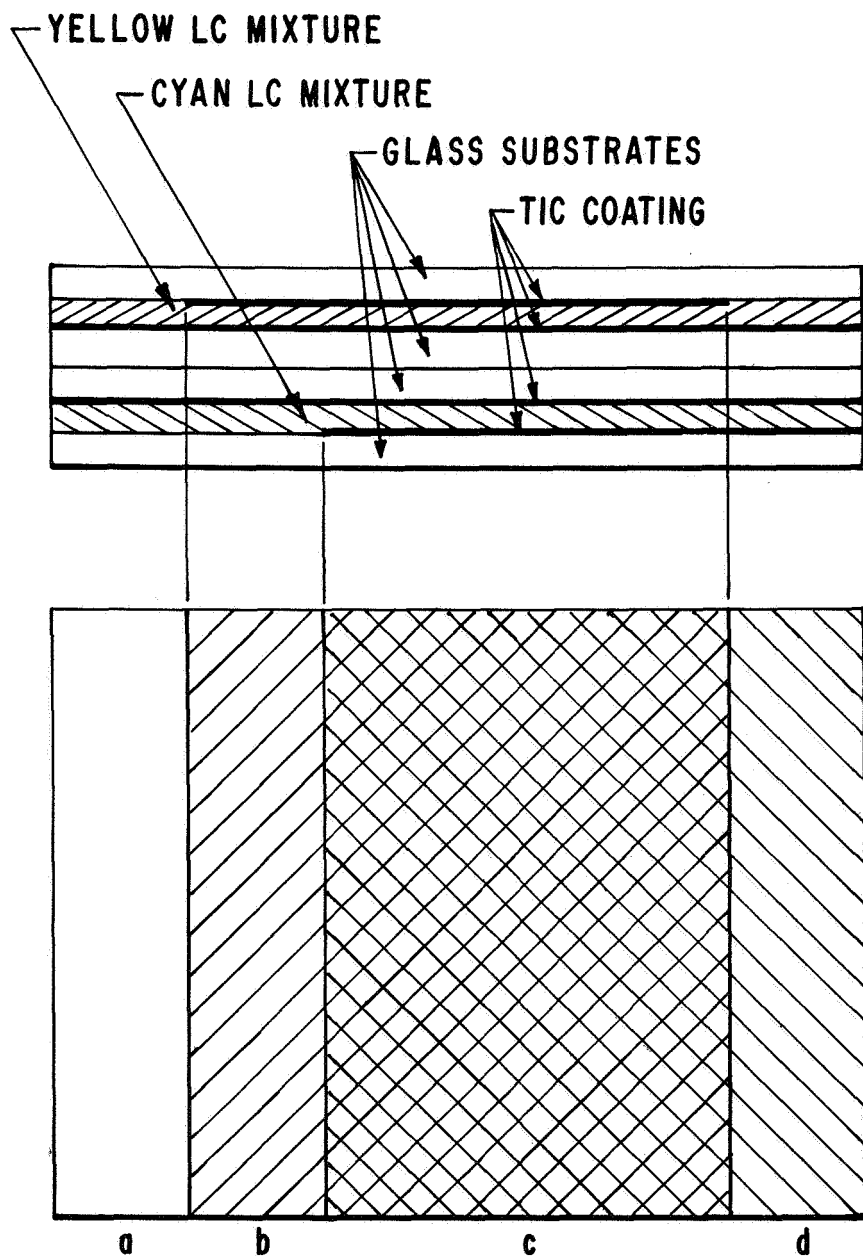
A state-of-the-art device which demonstrates these effects is shown in Figure 17. The difficulties encountered in fabricating a stable pleochroic magenta dye prohibited the fabrication of a completely controlled electronic optical filter. To illustrate the potential behavior of such a device, however, a plastic magenta filter strip (Kodak Wratten filter No. 32) was inserted between the cyan and yellow liquid crystal cells. The transparent conductive coating on each cell does not cover all the surface in contact with the dye-liquid crystal mixture. In this way it is possible to activate only certain portions of each layer and thus simultaneously produce a variety of color bands.

The drawing in Figure 18 is an example of the color patterns possible when both the yellow and cyan color cells are electronically activated. Along the plastic magenta filter strip, red and blue bands can be seen. At the left-hand corners of the cell, only the primary color green is visible. Similarly, other colors would be produced as indicated. The complete device is shown in the photograph of Figure 19. A schematic diagram of the electronic control circuit for this display is shown in Figure 20.

Some practical problems in the design and fabrication of this polychromic filter were encountered. As mentioned previously, the poor stability of the pleochroic magenta dye — liquid crystal mixture did not justify the complicated processing required for a three-layer color filter. Consequently, a separate 5.08-cm  $\times$  5.08-cm (2 in.  $\times$  2 in.) magenta color cell was fabricated using modified sealing techniques that, hopefully, will minimize this problem. In conjunction with the two-layer polychromic device, the magenta cell should offer color switching capabilities sufficient to demonstrate at least partially the color-selection characteristics of an electronically tunable optical filter.

A brief outline of some of the other more serious development problems is given below:

1. There is some doubt that a *single*-stacked unit can be fabricated that will be almost totally absorbing (black) with no electric field applied while maintaining the capability of transmitting "white" light with all three layers electronically activated. The maximum color contrast available from each of the colored layers is insufficient to allow such a broad range of color control. Also, the optical density and absorption characteristics of the composite color stack should compromise the spectral content of the illumination source and the spectral sensitivity of the average observer. Figure 21 illustrates the relative energy output of a "Daylight White" fluorescent lamp (used in our two-layer polychromic device) and the luminous efficiency of monochromatic radiant flux as a function of wavelength. The energy distribution of this lamp offers some partial correction for the decrease in eye sensitivity toward the red and blue portions of the color spectrum.



- a) - NO FIELD TO EITHER CELL
- b) - FIELD CAN ONLY BE APPLIED TO YELLOW CELL
- c) - FIELD CAN BE APPLIED TO BOTH CELLS
- d) - FIELD CAN ONLY BE APPLIED TO CYAN CELL

Figure 17. Top and edge view of two stacked color cells.

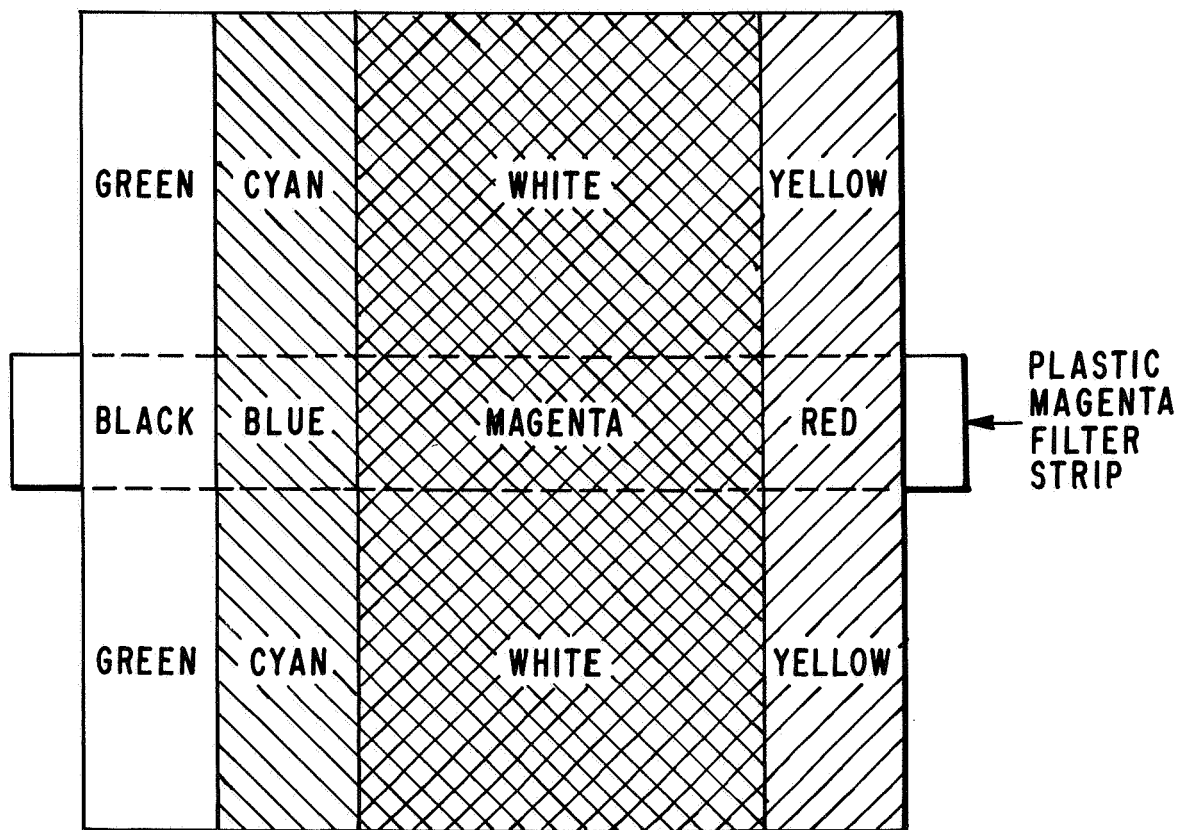


Figure 18. Color pattern of electronically activated two-layer polychromic filter.

2. Over a viewing area of a typical 3.5-cm  $\times$  3.5-cm display cell, it has been difficult to maintain acceptable color uniformity. This problem originates in the fabrication process and is a consequence of the necessity to align the pleochroic dye molecules in a fixed position relative to the incoming polarized light to allow the color characteristics of the dye molecules to be observed. This requirement allows the composite three-layer array to act as a series of polarizers and provides a simple means of observing even slight misalignment in material orientation as manifested by readily discernible color variations.
3. Since molecular orientation of the dye molecules is essentially a bistable condition due to the dielectric anisotropy of the host material, it is difficult to maintain a controlled orientation between maximum color absorption and maximum light transmission. Although this problem does not adversely affect the ability of the stacked layer to produce the primary additive and subtractive colors, electronic control of a full color spectrum is much more difficult.



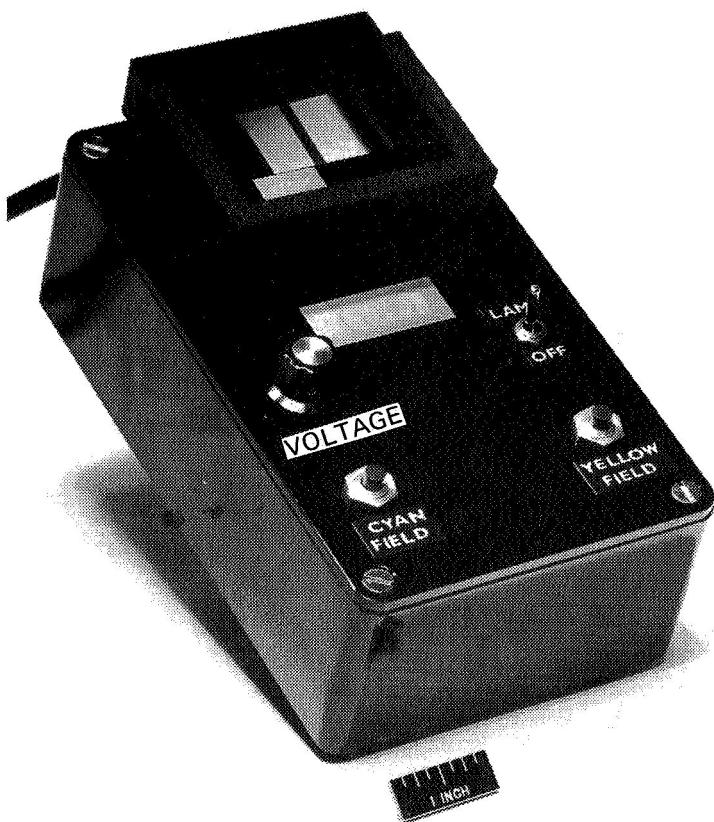


Figure 19.  
Two-layer electronically  
controlled color filter.

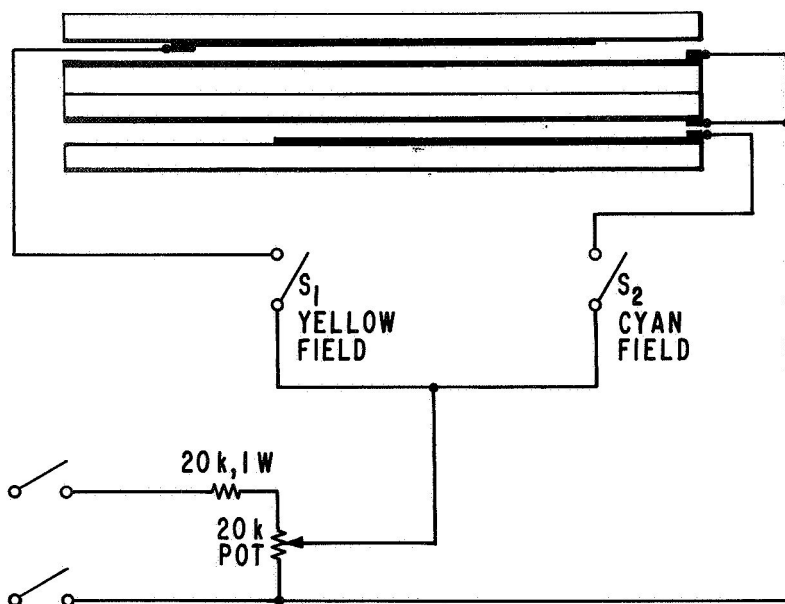


Figure 20.  
Schematic diagram of  
polychromic filter.

$S_1$  AND  $S_2$  - PUSHBUTTON SWITCHES

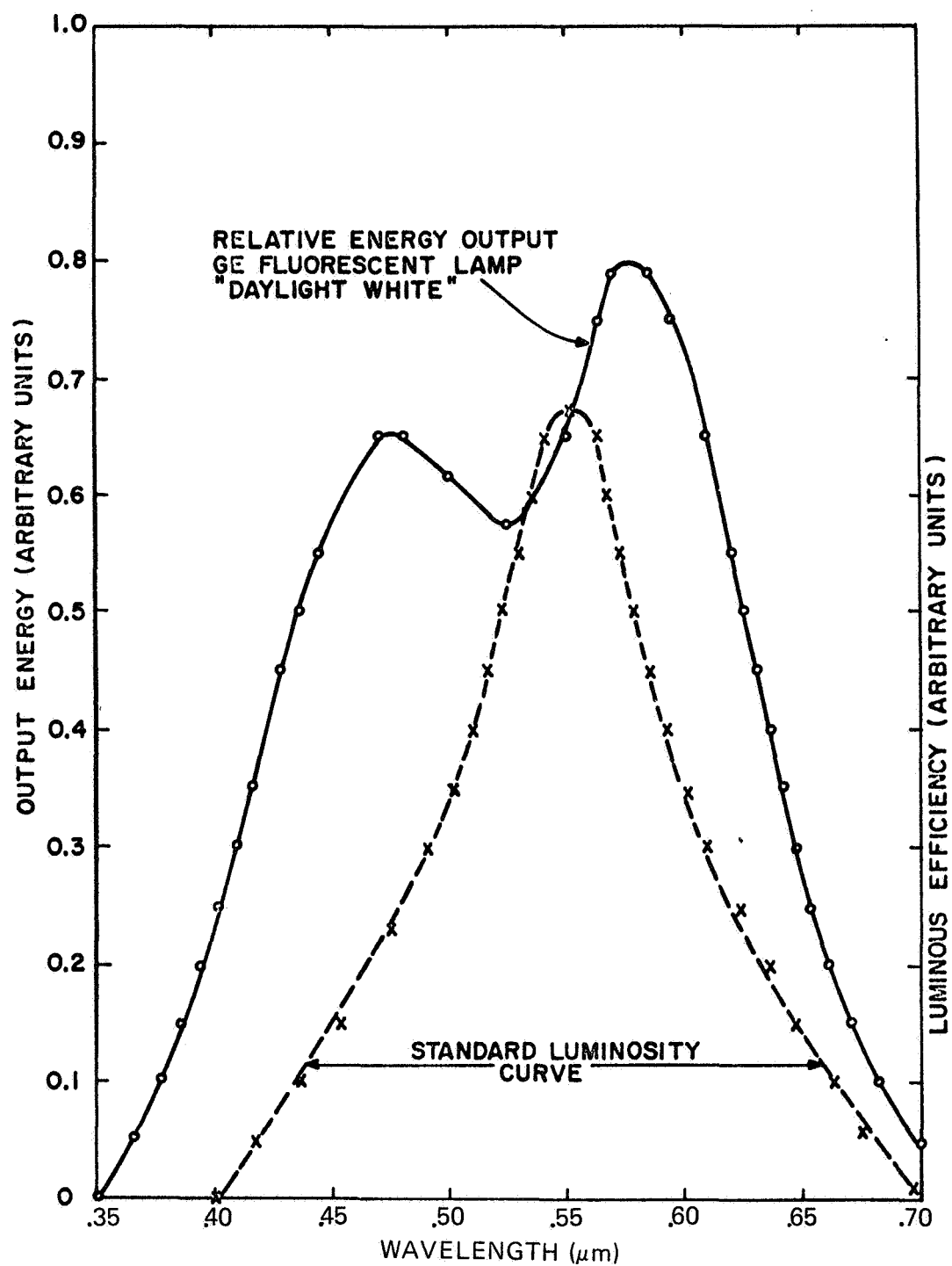


Figure 21. Relative radiant output energy and luminosity curves vs. wavelength.

Despite the efforts to minimize these problems, the final prototype model serves more to demonstrate these problems rather than the uniqueness of this electronic color filter. Considering the complexity of the fabrication process and the lack of immediate potential utility for this device, further development of the polychromic filter was minimized to devote experimental studies toward materials and devices exhibiting field-induced phase changes.

### B. Simulated Aircraft Engine-Monitoring System

One possible device using liquid crystal materials exhibiting the field-induced structure change might be a bar-graph display for aircraft or spacecraft instrument panels to provide a visual monitor of engine operating parameters. The concept of bar-graph displays has become a useful means for indicating selected operating conditions, especially where large numbers of flight conditions are to be simultaneously displayed on one panel. In such presentations, relative indications can be readily compared, rapid changes in information easily detected, and trends established if necessary.

To demonstrate the type of display a liquid crystal bar-graph device would present using materials exhibiting the field-induced phase change, the simple device illustrated in Figure 22 was fabricated. The basic structure of this device consists of two 10 cm x 10 cm glass plates in a parallel-plate configuration separated  $\sim 25 \mu\text{m}$  by insulating spacers. Capillary action is sufficient to constrain the selected liquid crystal mixture between the plates. A patterned transparent conductive coating was photoetched on the glass surfaces in contact with the liquid crystal mixture. On both glass plates, this patterned coating consists of three separate columns. However, on one of the glass surfaces the columns are segmented into twelve discrete areas with separate electrical contacts to each segment as shown in Figure 22.

The fixed numbers adjacent to each segment are arbitrary units representing a specific value of the parameter being monitored. For instance, each bar-graph might indicate either engine temperature, fuel pressure, or rpm. In multiengine aircraft, however, a more useful application of this bar-graph display might be to indicate the same operating parameter of three different engines simultaneously. Such a presentation would allow the pilot (or flight engineer) to quickly compare the relative condition of the engine function being displayed.

Figure 23 is a cross-sectional view of one of the segmented columns. Used in the reflective mode of operation, a thin layer of aluminum is evaporated on one of the glass substrates to either of the areas designated "A" and "B" in the illustration. Under high ambient light conditions, a circular polarizer could also be inserted (as shown) to improve contrast ratio. For a transmissive type of display, the aluminum reflective coating would

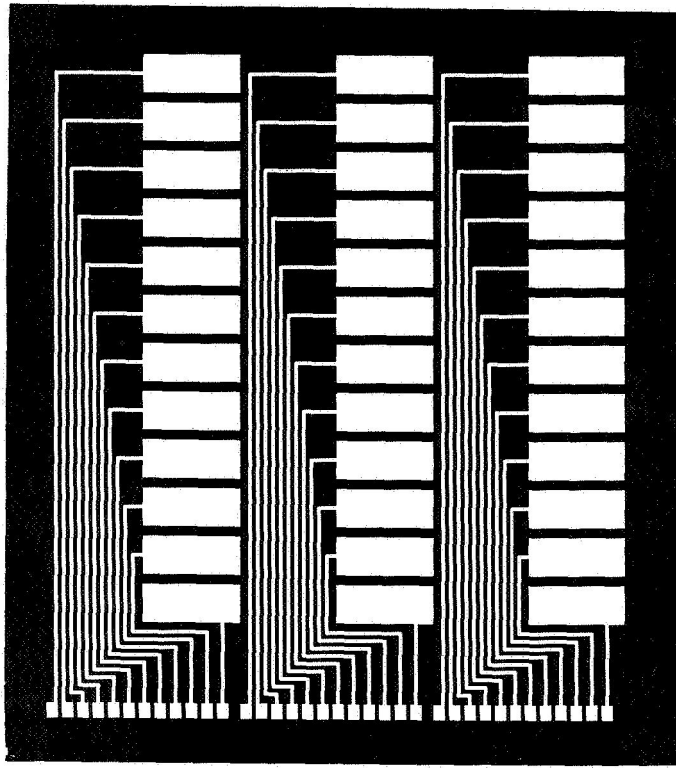


Figure 22.  
Top view of bar-graph display.

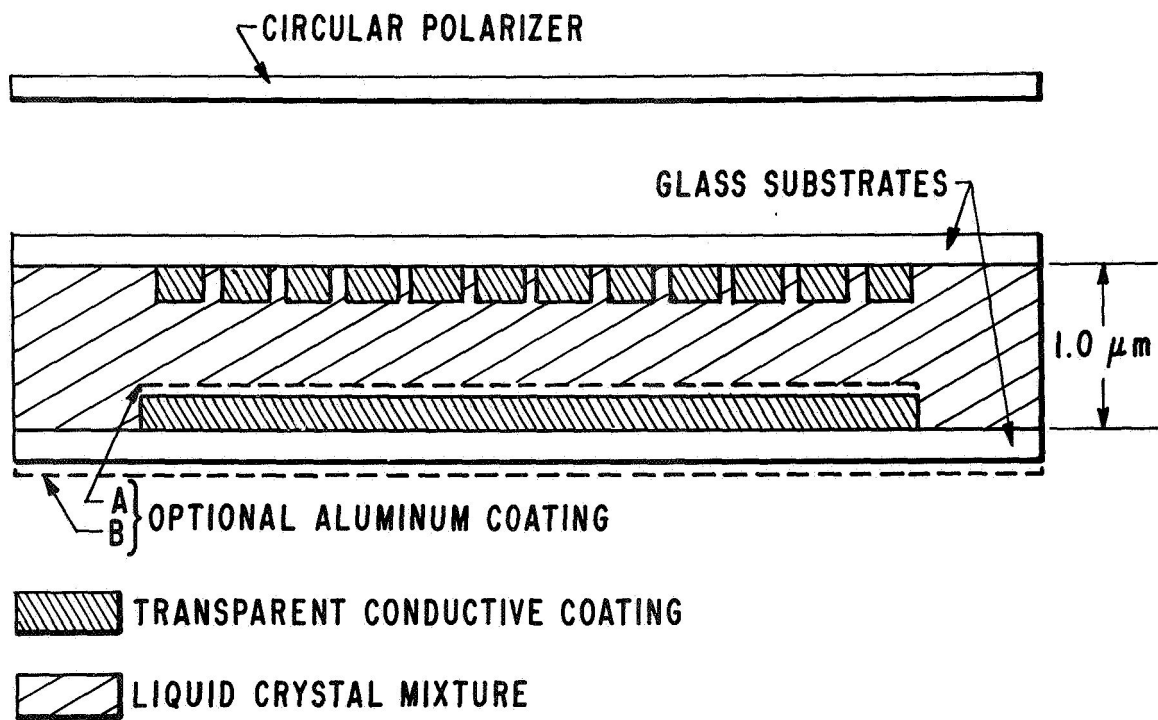


Figure 23. Cross-sectional view of segmented column.

be eliminated and a directional light source would illuminate the panel. The single circular polarizer could be replaced by crossed polarizers located at opposite ends of the liquid crystal device.

For this particular demonstration device, the separate elements in the bar-graph are selected by a continuously shorting rotary switch as shown in the schematic diagram of Figure 24. Each element can only be addressed by first activating in sequence those elements located below. For example, activation of the middle segments in any bar can only be accomplished by first activating the lower five (or six) segments of that bar. An alternate addressing scheme would be to activate only a single element so as to select a specific "window" in the bar-graph information display. The type of liquid crystal device (reflecting or transmitting) and the choice of associated electronic circuitry are options that are essentially dictated by the specific application of the monitoring indicators and lighting conditions of the entire display panel.

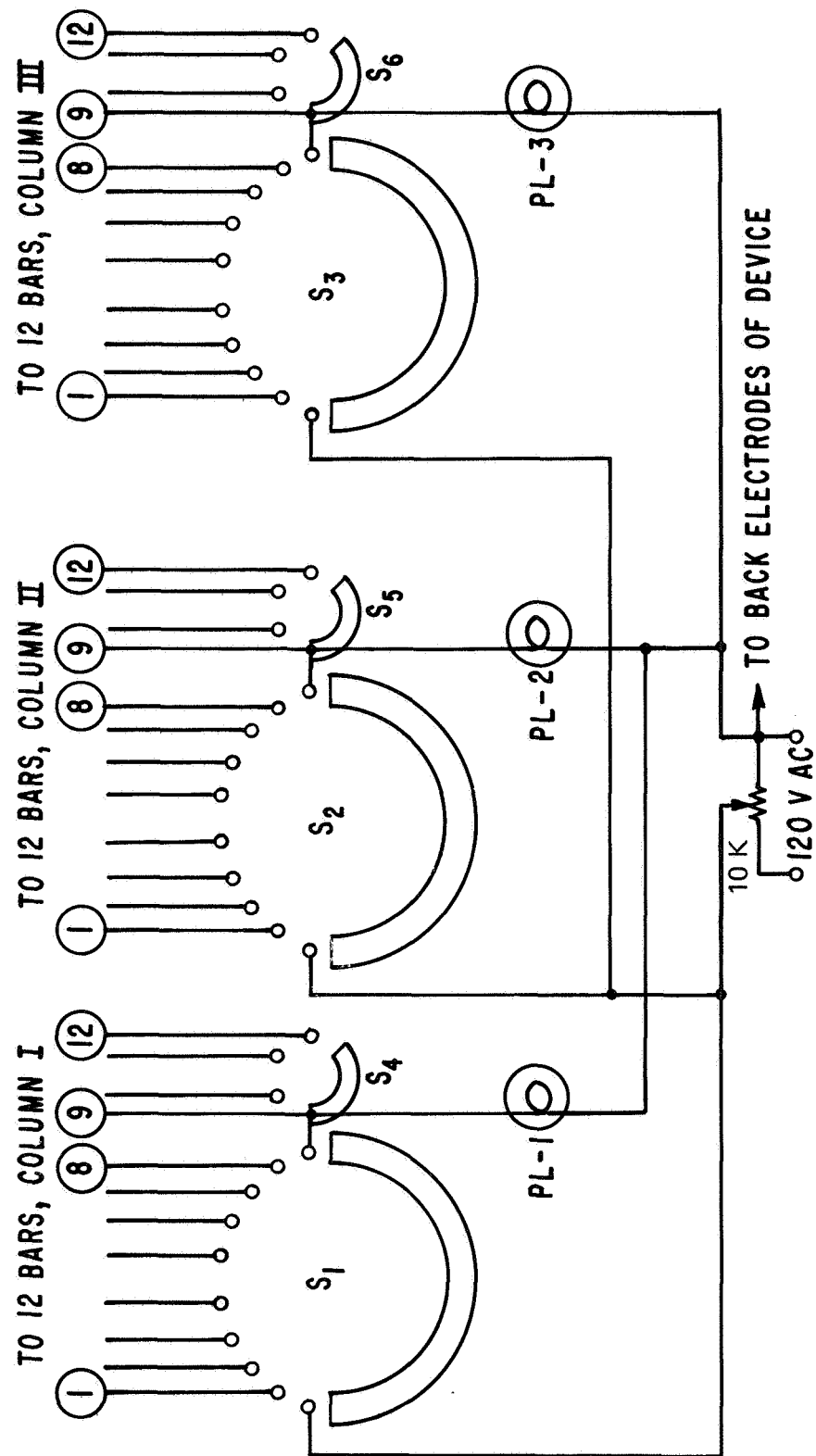


Figure 24. Electrical addressing scheme for 3-column bar-graph.

## REFERENCES

1. J. A. Castellano, E. F. Pasierb, G. H. Heilmeyer, and M. T. McCaffrey *Electronically Tuned Optical Filters*, Final Report, April 1969, Contract NAS 12-638.
2. J. A. Castellano, E. F. Pasierb, G. H. Heilmeyer, and M. T. McCaffrey, *Electronically Tuned Optical Filters*, Final Report, August 1970, Contract NAS 12-638.
3. J. J. Wysocki, J. Adams, and W. Haas, *Phys. Rev. Letters*, **20**, 1024 (1968).
4. G. H. Heilmeyer, L. A. Zanoni, and J. E. Goldmacher, *Liquid Crystals and Ordered Fluids*, Plenum Press, New York, 1970, p. 215.
5. D. L. Ross and E. Reissner, *J. Org. Chem.*, **31**, 2571 (1966).
6. J. A. Castellano, J. E. Goldmacher, L. A. Barton, and J. S. Kane, *J. Org. Chem.*, **33**, 3501 (1968).

## NEW TECHNOLOGY APPENDIX

### A. Electronically Tuned Neutral-Density Filter

*Brief Description:* An electronically tuned neutral-density filter was prepared with new non-steroidal cholesteric liquid crystals which have broad mesomorphic ranges.

*Detailed Description:* The new nonsteroidal compounds are optically active Schiff bases prepared by a multistep synthesis starting with a readily available optically active alcohol. Mixtures of these compounds have nematic Schiff bases, yield formulations which have broad cholesteric temperature ranges and relatively low viscosities, and require lower voltages than steroidal structures to produce electro-optical effects. Such formulations have a range from 0° to 75°C. This general class of materials was proposed and certain members of the class synthesized under RCA-funded work previous to, and outside of, the instant contract. Under the present contract several additional members of the class were synthesized for the first time. These materials may be used in electro-optic cells which can be electronically switched from an opaque to a clear state.

A 12.5- $\mu$ m-thick electro-optic cell (25 cm<sup>2</sup>) was prepared with the nonsteroidal cholesteric material described above. With no field applied only 5% of white light is transmitted through the cell while application of a  $2.5 \times 10^4$  V/cm electric field produces over 98% transmission. The 0.5-mil cell is turned on in  $\sim 100$  msec at 30 V, and relaxes to its original opaque state in 150 msec. Since this field-induced phase change is a field effect, very little power is consumed ( $\sim 1 \mu$ W/cm<sup>2</sup>).

*Applications:* Optical filters and information displays where power consumption must be minimized.

*Innovators:* J. A. Castellano, E. F. Pasierb, and C. S. Oh.

*Degree of Development:* Complete.

The above-described neutral-density filter is not believed to constitute an invention. Also, the additional members of the liquid crystal class synthesized hereunder are not believed to constitute invention over the precontract work.



## B. Aircraft Engine-Monitoring Indicator

*Brief Description:* A bar-graph display using the field-induced phase change materials described in A. above was fabricated.

*Detailed Description:* Bar-graph and window type displays are particularly suited to aircraft or spacecraft applications where changes in data rather than absolute values are of primary importance. Hence, a 100-cm<sup>2</sup> bar-graph display which simulates an aircraft engine-monitoring indicator was produced using the nonsteroidal cholesteric materials described above. The panel, which is completely opaque in its quiescent condition, consists of three bars, each having 12 elements. As each succeeding element in any one bar is activated, the material becomes clear and the engine operating parameter appears.

*Applications:* Aircraft instrumentation where low power and low cost are of primary importance.

*Innovator:* E. F. Pasierb.

*Degree of Development:* Complete.

The above-described aircraft engine-monitoring indicator is not believed to constitute an invention.